AD_____

AWARD NUMBER: W81XWH-05-1-0390

TITLE: Chemoprevention of Breast Cancer by Mimicking the Protective Effect of Early
First Birth

PRINCIPAL INVESTIGATOR: Malcolm C. Pike, Ph.D.

CONTRACTING ORGANIZATION: University of Southern California
Los Angeles, CA 90089

REPORT DATE: June 2009

TYPE OF REPORT: Annual

PREPARED FOR: U.S. Army Medical Research and Materiel Command
Fort Detrick, Maryland 21702-5012

DISTRIBUTION STATEMENT: Approved for Public Release;
Distribution Unlimited

The views, opinions and/or findings contained in this report are those of the author(s) and
should not be construed as an official Department of the Army position, policy or decision
unless so designated by other documentation.

REPORT DOCUMENTATION PAGE

Public reporting burden for this collection of information is estimated to average 1 hour per response, including the time for reviewing instructions, searching existing data sources, gathering and maintaining the data needed, and completing and reviewing this collection of information. Send comments regarding this burden estimate or any other aspect of this collection of information, including suggestions for reducing this burden to Department of Defense, Washington Headquarters Services, Directorate for Information Operations and Reports (0704-0188), 1215 Jefferson Davis Highway, Suite 1204, Arlington, VA 22202-4302. Respondents should be aware that notwithstanding any other provision of law, no person shall be subject to any penalty for failing to comply with a collection of information if it does not display a currently valid OMB control number. **PLEASE DO NOT RETURN YOUR FORM TO THE ABOVE ADDRESS.**

1. REPORT DATE	2. REPORT TYPE	3. DATES COVERED
1 June 2009	Annual	2 May 2008 – 1 May 2009

4. TITLE AND SUBTITLE

Chemoprevention of Breast Cancer by Mimicking the Protective Effect of Early First Birth

5a. CONTRACT NUMBER

5b. GRANT NUMBER
W81XWH-05-1-0390

5c. PROGRAM ELEMENT NUMBER

6. AUTHOR(S)

Malcolm C. Pike, Ph.D.

E-Mail: mcpike@usc.edu

5d. PROJECT NUMBER

5e. TASK NUMBER

5f. WORK UNIT NUMBER

7. PERFORMING ORGANIZATION NAME(S) AND ADDRESS(ES)

University of Southern California
Los Angeles, CA 90089

8. PERFORMING ORGANIZATION REPORT NUMBER

9. SPONSORING / MONITORING AGENCY NAME(S) AND ADDRESS(ES)
U.S. Army Medical Research and Materiel Command
Fort Detrick, Maryland 21702-5012

10. SPONSOR/MONITOR'S ACRONYM(S)

11. SPONSOR/MONITOR'S REPORT NUMBER(S)

12. DISTRIBUTION / AVAILABILITY STATEMENT
Approved for Public Release; Distribution Unlimited

13. SUPPLEMENTARY NOTES

14. ABSTRACT

We have successfully shown that in the rat estradiol, estradiol plus progesterone, and beta-HCG is protective against carcinogen-induced mammary tumorigenesis; treatment and pregnancy induced RNA gene expression changes in the breast have been identified. Analysis of gene expression differences in the breast of parous and nulliparous women undergoing elective reduction mammoplasty has begun. Estrogen receptor, progesterone receptors and cell proliferation in the breast has been characterized (by immunohistochemistry, IHC) in parous and nulliparous women and in breast tissue obtained in the first trimester of pregnancy. RNA characterization of these samples has begun. Four protocols providing information related to chemoprevention have been developed – these investigate breast cell proliferation, receptor IHC and gene expression: (1) the effect of high dose progestin exposure, recruitment ongoing; (2) the effect of oral contraceptive progestin dose, recruitment complete, IHC being analyzed; (3) the effect of high dose estrogen exposure, recruitment complete, IHC being analyzed; and (4) the effect of natural progesterone exposure, recruitment complete. Pregnancy reduces mammographic density and breast cancer risk. How these are related has been studied in a large autopsy series; results suggest that part of the protection may be the result of a reduction in breast epithelium; further studies of these samples are ongoing.

15. SUBJECT TERMS
No Subject Terms provided.

16. SECURITY CLASSIFICATION OF:			17. LIMITATION OF ABSTRACT	18. NUMBER OF PAGES	19a. NAME OF RESPONSIBLE PERSON USAMRMC
a. REPORT	b. ABSTRACT	c. THIS PAGE			19b. TELEPHONE NUMBER *(include area code)*
U	U	U	UU	53	

Table of Contents

INTRODUCTION: This Innovator Award is designed to provide insight into the ways in which a chemoprevention regimen can mimic the protective effect of a full-term pregnancy (a birth) against breast cancer. In addition, we are aiming to understand the mechanisms underlying the risk associated with increased mammographic density, the strongest known risk factor for breast cancer after the highly penetrant genetic risk factors of BRCA1 and BRCA2 mutations. Mammographic densities are permanently reduced by births; and this relationship is being explored to determine if this is an important part of the mechanism by which births provide protection against breast cancer. This work is being conducted both in humans and rodents.

BODY: The Innovator Award consists of four projects (Projects 1 and 2 are being completed through a subcontract to our colleague Dr. Lewis Chodosh at the University of Pennsylvania, and Projects 3 and 4 are being completed by the team at USC).

Projects 1 and 2

Task 1: Months 1-12: Treat rats with different hormonal chemoprevention regimens, harvest mammary tissue, and isolate RNA.

   As described in the Year 3 Progress Report, this task was completed on schedule.

Task 2: Months 6-24: Analyze morphological changes and determine global gene expression profiles for rat mammary gland samples from rats treated with different hormonal chemoprevention regimens.

   In the last Progress Report we described our efforts aimed toward identifying genes whose expression changes in response to both pregnancy and protective, but not non-protective, hormonal treatments. In this manner we identified a list of genes whose expression increases (up-regulated genes) or decreases (down-regulated genes) in response to pregnancy and protective hormone treatments.
   We next wished to assess the overlap between these lists and the gene signature ('core parous signature') that we identified as being conserved across multiple rat strains, as is described in Tasks 3 and 4. We focused our initial efforts on genes that are up-regulated in response to parity or protective hormone treatments. The core parous signature contains 17 up-regulated genes, and there are 39 genes whose expression is commonly up-regulated among protective hormonal treatments. There is a statistically significant overlap of 8 genes between these two lists ($p < 1 \times 10^{-10}$, hypergeometric test).
   The core parous signature was identified by comparing gene expression changes common across several rat strains, while the protective hormone signature was generated in Lewis rats. When we limited our analysis to Lewis rats, the intersection of the lists increased to 23 of the 39 genes ($p < 1 \times 10^{-12}$).
   Global analysis of gene expression using principal component analysis (PCA) revealed that hCG treatment elicited distinct gene expression changes as compared to pregnancy, E, or E+P (Fig. 1). Thus we considered that eliminating hCG from the analysis might further increase the overlap between the two signatures. Indeed, comparing only genes altered in response to pregnancy, E, and E+P with the Lewis-only signature described above yielded the most significant overlap ($p < 1 \times 10^{-16}$).
   These results suggest that gene expression changes that are a common end-point of

4

protective hormonal changes are very similar to pregnancy-induced changes that are conserved across multiple rat strains.
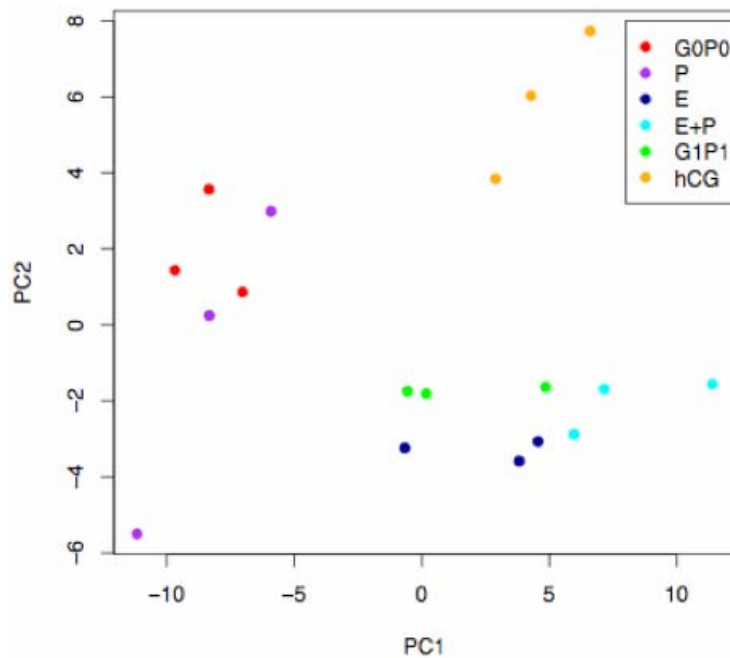

Figure 1. Principal component analysis of hormonal treatments or pregnancy showing that hCG elicits distinct gene expression patterns compared to other protective conditions.

Task 3: Months 6-36: Identify genes that are expressed in a parity-specific manner in the rat.

As described in the Year 3 Progress Report, this task was completed on schedule, and these results published (Blakely et al., 2006; erratum 2007).

Task 4: Months 6-36: Identify genes whose expression in rats correlates with protection against breast cancer.

As described in the Year 3 Progress Report, this task was completed on schedule.

Task 5: Months 1-48: Isolate RNA from human mammary gland samples and control epithelial and stromal samples.

Per the SOW, this task was completed on schedule. RNA has been isolated from a large number of the available human specimens. In addition, we have prepared RNA from control samples consisting of: intact adipose tissue, intact fibrous (i.e. stromal and epithelial) breast tissue, epithelial organoids isolated by collagenase digestion, cultured epithelial organoids, and cultured fibroblasts from reduction mammoplasty specimens.

To achieve the objectives of this aim, we have collected 168 snap-frozen human breast samples (43 nulliparous, 125 parous) from patients who had either undergone

5

reduction mammoplasty or had an excisional biopsy for a lesion that was ultimately determined to be benign (and not associated with elevated breast cancer risk). Tissue was taken from regions determined to be normal, as assessed by a breast pathologist. Women providing samples were interviewed to obtain information on age at the time of biopsy, age at first full-term pregnancy, age at last full-term pregnancy, number of pregnancies, number of live births, spacing of live births, lactation history, ages at first miscarriage or abortion, total number of miscarriages and abortions, menopausal status, age at menopause, history of bilateral oophorectomy, history of oral contraceptive use, and history of postmenopausal hormonal replacement therapy. Of the 168 frozen samples that we received from the Mayo Clinic, we found adequate reproductive information for 90 samples (64 parous, 26 nulliparous). Age of individuals ranged from 20-79 (median 41) and age at FFTP for parous samples ranged from 16-35 (median 23). RNA was harvested from these samples and its integrity was assessed. We obtained high-quality, intact RNA from 86 samples (60 parous, 26 nulliparous) for subsequent Affymetrix microarray analysis.

In an effort to perform 'expression deconvolution' on our existing data set, we generated a reference data set derived from the various cell types within the breast. We obtained fresh human samples from reduction mammoplasties immediately following surgery. Pieces of tissue were dissected grossly to yield regions enriched for adipose, fibrous tissue, and epithelium (Fig. 2). Additional pieces of fibrous-rich tissue were digested with collagenase, and subject to centrifugation and filtration. Cultures of pure epithelial and fibroblast cells were obtained from flow-thru filtration columns and passaged in culture. Epithelial rich digested organoids were also obtained during the filtration process. Finally, from each mammoplasty we were able to isolate adipose, fibrous, digested organoid and pure populations of epithelial and fibroblast cells from tissue culture. RNA was extracted from each of these reference populations for subsequent Affymetrix microarray analysis.
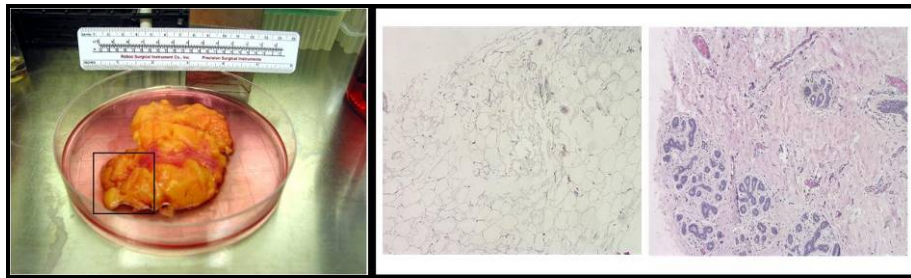

Figure 2. Representative sample from a reduction mammoplasty obtained immediately post-surgery (left). Hematoxylin and Eosin stained sections derived from tissue enriched for adipose (center) and fibrous tissue (right).

Task 6: Months 3-52: Determine global gene expression profiles for human mammary gland samples using oligonucleotide microarrays.

Per the SOW, this task has been completed ahead of schedule. Tissue samples with sufficient RNA yields and quality were labeled according to manufacturer's protocol for hybridization to Affymetrix U133A GeneChips. Following labeling and hybridization to microarrays, 72 samples (50 parous, 22 nulliparous) passed QC inspection and were

appropriate for analysis. For the isolated tissue compartments, we profiled each of the cellular compartments for 8 independent reduction mammoplasties on Affymetrix U133A GeneChips.

The experiments conducted in this Task have provided us with gene expression data on a large number of human breast samples with known reproductive history, as well as the expression profiles of isolated tissue compartments from the human breast. Together, these data will allow us to identify gene expression changes that correlate with reproductive status, while using the reference data set to correct for changes in epithelial content among samples. These efforts are described in Task 7.

Task 7: Months 12-60: Identify genes whose expression in the mammary gland in women reflects aspects of reproductive history that impact on breast cancer susceptibility.

Per the SOW, work on this task is continuing on schedule. Preliminary results have suggested that identifying genes whose expression correlates with reproductive history may be confounded by significant variations in epithelial content among breast samples. Below we discuss these results and our attempts to overcome this technical difficulty.

As a preliminary approach toward completing this task, we explored the use of principal component analysis (PCA) to provide an overview of these samples. PCA uses the most variant genes in a dataset (~6700 for this dataset), and projects samples within a virtual three dimensional space based on gene expression. The first two components typically reflect the most robust differences in gene expression among samples. Breast samples for nulliparous (green) and parous (pink) microarrays did not appear to be distinguishable on the basis of the first two components by PCA (Fig. 3). This finding suggests that reproductive history does not explain the most predominant inter-patient differences in gene expression. Incidentally, in analogous studies using rodent samples, parity-induced gene changes typically predominant the first two components of a PCA, rendering nulliparous and parous samples into unique gene expression space.
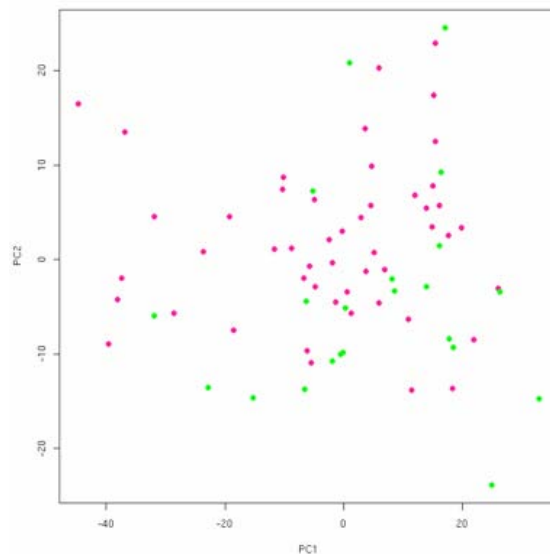

Figure 3: Principal Component Analysis based on the expression of ~6700 variant probe sets demonstrates that nulliparous (green) and parous (pink) samples do not separate by the first 2 components, suggesting that reproductive history is not the largest discriminator for this data set.

7

In light if this finding, we sought to identify the genes that contribute to the first and second components of the PCA. Gene markers characteristic of epithelial cells or epithelial content appeared to constitute the predominant pathway identified. Based on this information, we then coded the samples by high (red) to low (blue) epithelial gene expression using PCA analysis, and confirmed that the pattern observed for the Mayo data set can be explained by the relative epithelial content in the original frozen samples (Fig. 4). Unfortunately, this technical variability confounded our ability to address gene expression changes based on reproductive history. To circumvent these issues, we proposed using a mathematical approach termed "expression deconvolution." Past experience dictates that the interpretation of gene expression data derived from complex organs composed of multiple cell types (like the breast) is complicated by the fact that observed changes in gene expression may be due either to cell-intrinsic changes in gene expression or to changes in the relative abundance of different cell types. Consequently, *bona fide* changes in intrinsic gene regulation can either be mimicked or masked by changes in the relative proportion of different cellular compartments. Therefore, we sought to generate reference expression data from purified populations of constituent cell types within the mammary gland, and use this information to computationally adjust for differences in cellular compartments within samples.
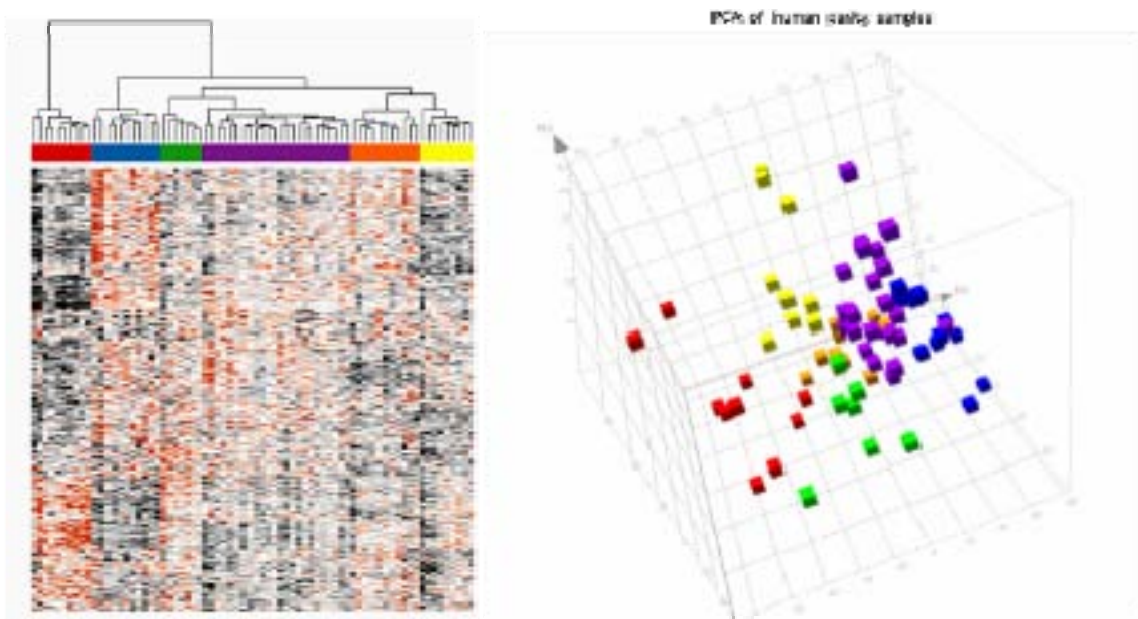

Figure 4. Hierarchical clustering of gene expression data derived from the 72 normal human breast tissue samples demonstrates that epithelial content of the individual samples drives expression to a greater extent than does reproductive history (left). Principal component analysis of individual samples color coded for high expression of epithelial genes (red) to low expression (blue).

As described in Task 5 above, we generated RNA from purified epithelial, adipose, and fibrous tissue from reduction mammoplasties to serve as a reference for compartment adjustment, and profiled each compartments from 8 samples on U133A Affymetrix GeneChips. Samples passing QC were subsequently analyzed by PCA using ~5700 genes with high variance across the data set. With the exception of two adipose samples (which likely contained undetectable fibrous contamination), all cellular subtypes were

distinguishable by PCA. Moreover, cell types that were maintained in culture (epithelial and fibroblast) appeared to be distinct from the uncultured tissues obtained from gross dissection (Fig. 5). As a first pass at defining genes that would be good discriminators of compartment class, we compiled lists of genes that were unique to adipose, cultured epithelial cells and cultured fibroblasts. Going forward, these lists of genes will serve as reference datasets that should enable us to estimate the proportion of each cellular compartment present within a complex mixture of cell types. We will use these datasets and apply a mathematical model to our human Mayo samples to predict tissue compartment content. This approach will allow us to correct for changes in epithelial content among samples, and may thereby allow for the discovery of genes that correlate with reproductive history. These studies will be executed in the final study period.
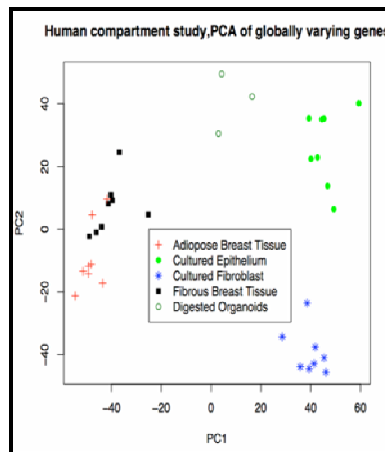

Figure 5. Principal Component Analysis of tissue compartments isolated from human reduction mammoplasties demonstrate almost complete separation by tissue type using ~5700 genes with high variance.

Task 8: Months 1-36: Determine the effect of short-term, low-dose estradiol and progesterone treatment on MNU-induced mammary tumor susceptibility.

    As described in the Year 3 Progress Report, this task was completed on schedule.

Task 9: Months 12-60: Determine the effect of hormone treatment on MNU-induced mammary epithelial proliferation.

    This task has been temporarily delayed to allow for progress toward and completion of other tasks. Work on this task will continue during the next study period, consistent with the SOW.

Task 10: Months 12-60: Determine whether p53 loss abrogates pregnancy-induced protection against carcinogen-induced mammary tumorigenesis.

    This task has been initiated and is proceeding according to the SOW. In order to address this aim, we first needed to demonstrate that the hormone-induced protection

against tumors that has been observed in rats is also operative in mice. This is because mice, but not rats, offer the opportunity to use genetic knockouts, which is the preferred approach for addressing the involvement of p53 in pregnancy-induced protection.

During the previous study period we performed a number of experiments to determine whether mice also exhibit hormone-induced protection. We tested multiple strains—BALBc/J mice, which have been shown by the Medina lab to be afforded protection by hormone treatment, and FVB mice, which is the strain used for many knockout studies in many laboratories, including our own. We tested BALBc/J mice from a commercial source as well as a BALBc/J substrain obtained directly from the Medina lab. We also tested whether hormone treatment can delay tumorigenesis initiated by the Neu oncogene in MMTV-Neu. As described in last year's report, E+P treatment did not delay mammary tumorigenesis in any of these experiments.

This result was unanticipated, given that the Medina lab had previously demonstrated that E+P treatment confers protection in BALBc mice. We reasoned that endogenous phytoestrogens present in the mice's diet may be confounding these experiments by altering the hormonal milieu of the mice. To address this issue, we tested whether mice that were maintained on a low phytoestrogen diet exhibited hormone-induced protection. Breeders were fed the low phytoestrogen diet AIN-76 Blue at the time of mating, and female offspring were used for tumorigenesis experiments. Experimental animals were also fed AIN-76 Blue at weaning and throughout the course of the experiments. Mice were treated with estrogen plus progesterone (E+P) for 21 days beginning at 7 weeks of age, followed by DMBA administration from 12 to 18 weeks to induce tumorigenesis.

The results of this experiment showed that E+P treatment caused a modest delay in mammary tumorigenesis (Fig. 6). However, interpretation of these results was hampered by the high mortality induced by DMBA in this experiment. Experiments to confirm this preliminary result, and circumvent this problem, will be conducted in the next study period.
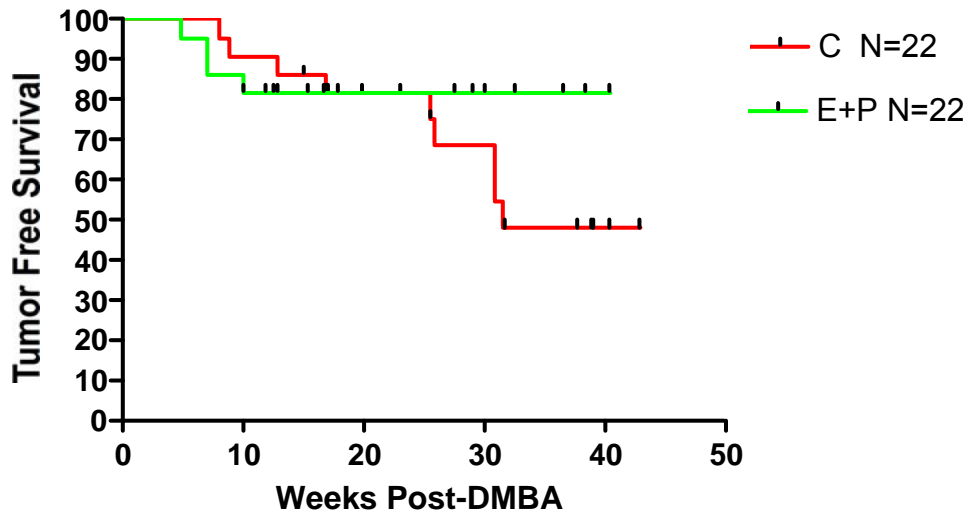

Figure 6. E+P treatment confers a modest delay in DMBA-induced mammary tumorigenesis in BALBc/J mice on a low phytoestrogen diet.

In light of the potential protection conferred by E+P treatment when mice are fed a

low phytoestrogen diet, we next tested whether E+P could delay tumorigenesis in MMTV-Neu mice on this diet. MMTV-Neu mice fed AIN-76 Blue were treated with E+P or cellulose control at 7 weeks of age for 21 days, and then monitored for tumor formation. Unlike with DMBA-induced tumorigenesis, E+P treatment did not delay tumorigenesis in MMTV-Neu mice, even when fed a low phytoestrogen diet (Fig. 7). This suggests that this experimental paradigm may not be suitable for studying parity- or hormone-induced protection in mice.

In the final study period, we will attempt to confirm the preliminary finding that hormone treatment may only confer protection against mammary tumorigenesis when mice are fed a diet with low phytoestrogens. If this finding can be repeated, we can then test whether p53 loss abrogates this protection by performing this experiment in p53-null BALBc mice. These experiments will provide important insights into the mechanism of parity-induced protection in rodents and humans.
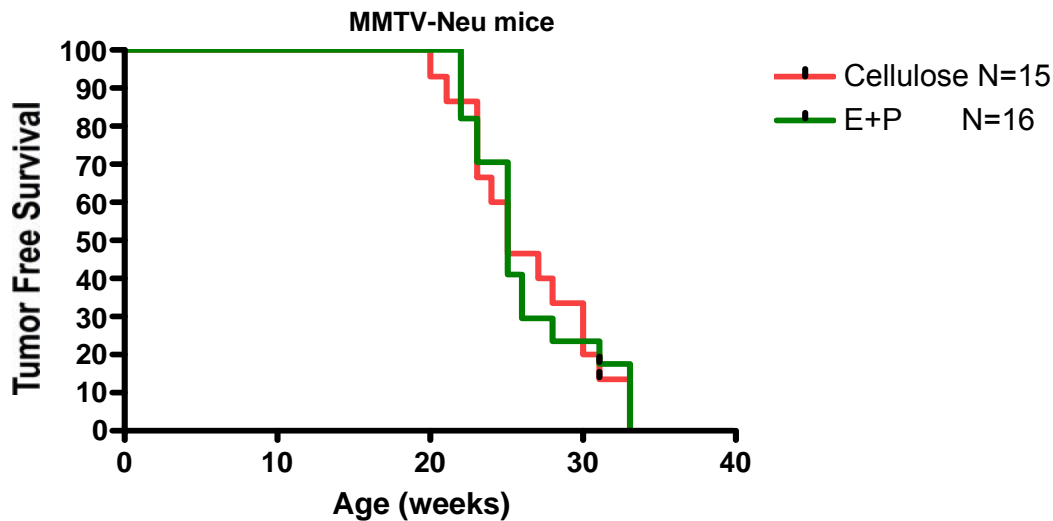

Figure 7. E+P treatment does not delay MMTV-Neu-induced mammary tumorigenesis in mice fed a low phytoestrogen diet.

Project 3

This project aims to recruit subjects being treated with a variety of hormonal regimens to have pre- and/or post-treatment breast biopsies. The treatment with the hormonal agents may or may not be a study procedure. A number of cellular, hormonal and genetic analyses will be carried out on the biopsy specimens.

Task 1. Months 1-48: Develop appropriate protocols and treatment regimens.

Completed.

Task 2. Months 24-56: Recruit subjects to the treatment protocols.

Task 2a. Recruit 10 women receiving high dose progestin (Megace) for the treatment of endometrial hyperplasia (as standard of care). For this research protocol, the subjects will receive a breast biopsy before Megace treatment, and after

three months of Megace treatment.

For various reasons, including the relocation of USC/Los Angeles County (USC/LAC) Women's Hospital to a new facility, this has been a difficult protocol as regards recruitment. We have consented five subjects for this protocol, three of whom have completed. We have recruitment procedures in place and, with the active involvement of a new Ob/Gyn fellow, we expect to complete enrollment in the next six months.

Task 2b. Recruit 40 women seeking oral contraceptives to be randomized to a low-dose progestin content oral contraceptive or a standard progestin content oral contraceptive and to have a breast biopsy after three months of oral contraceptive use.

Completed.

Task 2c. Recruit 36 women receiving Depot Medroxy-progesterone Acetate (DMPA) as part of standard of care. For this research protocol, the subjects will receive a breast biopsy on day 7 ± 1, day 14 ± 1 or day 21 ± 1 (12 subjects on each of these three days) after their 2nd or subsequent consecutive DMPA injection.

This protocol will augment Task 2a as it measures the effect of high levels of progestins. Recruitment will begin using alternative funding mechanisms while we await DOD IRB approval; the protocol is being submitted to the DOD IRB within the next two weeks. We plan to recruit at the Family Planning Clinic at USC/LAC Hospital as well as through advertisements and we have made contact with the Avon/Love Army of Women which, we are hopeful, will lead to substantial volunteer recruitment.

Task 2d. Recruit 50 volunteer women who are not pregnant and not currently receiving any hormonal agents to undergo a breast biopsy. This protocol will specifically recruit women into the following categories: premenopausal, nulliparous – under the age of 30 (5 women)/over the age of 30 (5 women); premenopausal, parous – under the age of 30 (10 women)/over the age of 30 (5 women); and postmenopausal – nulliparous (15 women)/parous (10 women).

Recruitment will begin using alternative funding mechanisms while we await DOD IRB approval; the protocol is being submitted to the DOD IRB within the next two weeks.

Task 3. Months 30-58: Assay tissue samples* for cellular, hormonal and gene expression markers to determine pre- and/or post-treatment tissue characteristics.

We have completed or are currently looking at MIB-1, ER, PR-A and PR-B by immunohistochemistry (IHC) in the samples. Additional IHC for apoptosis is ongoing. We are currently carrying out laser capture microdissection (LCM) on these tissues in an attempt to obtain separate epithelial and stromal cell populations. LCM has proven to be

a major challenge. Adequate amounts of RNA have been obtained from the samples but the RNA quality has not been adequate for Affymetrix analysis; this has also been a major problem in the rat work described in Projects 1 and 2 above, and has also been a problem for other investigators working with human breast tissue. The RNA from whole tissue has been of adequate quality but we believe that pure cell populations may be necessary if we are to understand what changes are truly important. To this end we are currently investigating the new technologies that do not require such high quality RNA, namely, the Illumina DASL approach and the NanoString approach. There is good evidence that these approaches may also work well with standard formalin-fixed tissue.

Task 4. Months 30-58: Assay blood samples* for hormone levels.

We have provided the blood samples to the lab and this work is in process.

Task 5. Months 30-60: Conduct data analysis* to compare pre- and/or post-treatment tissue characteristics, to compare these changes to the differences noted between nulliparous and parous women, and to prepare manuscripts as appropriate.
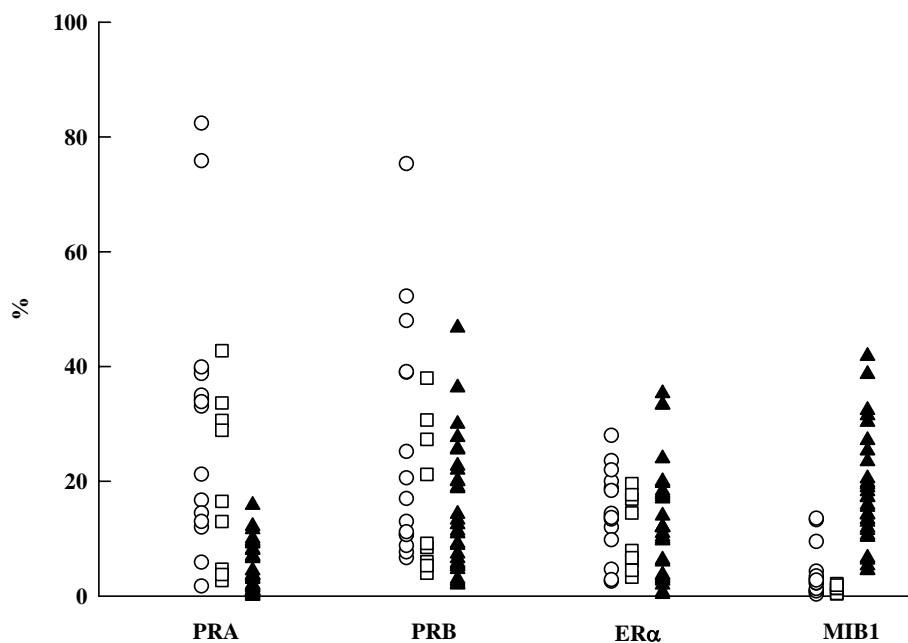

Fig. 1 % of cells expressing nuclear PRA, PRB, ERα and MIB1 in premenopausal nulliparous (○), premenopausal parous (□) and pregnant (▲) women.

Figure 8. Figure 1 from Taylor et al. (2009).

We have published a manuscript (Taylor et al., 2009; attached) which compares cellular markers in the tissue collected as part of Project 4 with 'pregnant' breast tissue (see below). This manuscript reported our studies of nuclear staining for the

progesterone and estrogen receptors (PRA, PRB, ERα) and cell proliferation (MIB1) in the breast terminal duct lobular unit (TDLU) epithelium of 26 naturally cycling premenopausal women and 30 pregnant women (median 8.1 weeks gestation). Results are shown in Figure 8. PRA expression decreased from a mean of 17.8% of epithelial cells in cycling subjects to 6.2% in pregnant subjects ($P = 0.013$). MIB1 expression increased from 1.7% in cycling subjects to 16.0% in pregnant subjects ($P < 0.001$). PRB and ERα expression were slightly lower in pregnant subjects but the differences were not statistically significant. Sixteen of the non-pregnant subjects were nulliparous and ten were parous. PRA was statistically significantly lower in parous women than in nulliparous women (32.2% in nulliparous women vs 10.2%; $P = 0.014$). PRB (23.5 vs 12.9%), ERα (14.4 vs 8.6%) and MIB1 (2.2 vs 1.2%) were also lower in parous women, but the differences were not statistically significant. PRA expression may be a most useful marker of the reduction in risk with pregnancy and may be of use in evaluating the effect of any chemoprevention regimen aimed at achieving a similar reduction in risk. Short-term changes in PRA expression while the chemoprevention is being administered may also be an important marker (see results of the preliminary analysis of the results of Task 2b below). A most important aspect of these findings was that the marked decreases in PRA in pregnancy and in parous women have also been found in the rat. This lends much credence to the rat model for studying the protective effect of pregnancy, and suggests that the gene changes found in the rat (Projects 1 and 2 above) may be directly applicable to the human situation.

We are preparing a manuscript describing the results of Task 2b. Task 2b was a randomized trial comparing the effects on breast tissue of two FDA approved and commonly prescribed oral contraceptives (OCs) – OrthoNovum 1/35 and Ovcon 35. These two OCs both contain 35 µg of the estrogen, ethinyl-estradiol (EE_2), but different doses of the progestin, norethisterone (NET) – OrthoNovum 1/35 contains 1 mg of NET while Ovcon 35 contains 0.4 mg NET. The hypothesis being tested was that Ovcon 35 would be associated with a much lower level of breast cell (TDLU) proliferation than OrthoNovum 1/35 based on its lower level of progestin. We had previously shown based on the results of studies of the increased breast cancer risk from use of menopausal estrogen/progestin therapy that this difference in dose was in the significant dose-effect range of NET (Lee et al., 2005). The results of the study and comparison to our published results (Fig. 8) are shown in Figures 9 and 10. In direct contrast to expectation, the lower dose OC, Ovcon 35, was associated with greater TDLU cell proliferation as measured by MIB1 than OrthoNovum 1/35 (median values of 14% and 7%; Fig. 9). The cell proliferation with both OCs was higher than was seen in normally cycling women, and that of Ovcon 35 approached that seen in pregnant women in the first trimester (Fig. 8). Figure 10 shows that these OCs also affected PRA expression in the direction of pregnancy. These results are quite extraordinary and demand a complete rethinking of how OCs affect the breast if these results are confirmed in additional investigations. One possibility for the lower cell proliferation with the higher dose OC is via androgens. OCs suppress ovarian steroid production including androgens in a dose dependent manner and there is evidence that a substantial amount of estrogen in normally cycling women is metabolized in the breast from androgens. It is just possible that there is a lower level of estrogen within the breast with a higher dose OC. It is not at all clear why PRA should

be affected towards a pregnant state. We are currently determining how we will pursue these results further.

Figure 9. TDLU proliferation rates as measured with MIB1 in naturally cycling and first trimester pregnant women, as well as women using two oral contraceptives (Ovcon 35 and OrthoNovum 1/35).

Figure10. TDLU PRA expression in naturally cycling and first trimester pregnant women, as well as women using two oral contraceptives (Ovcon 35 and OrthoNovum 1/35).

* The tissue and blood assays as well as the subsequent data analysis include specimens (including breast biopsies) collected on protocols funded via other mechanisms that directly relate to this Innovator Award. These include specimens from: (1) 33 women undergoing a termination of pregnancy - breast biopsy obtained immediately after the termination and a subsequent biopsy several months later (a source of non-pregnant tissue). This protocol was aimed at measuring the effects of pregnancy levels of high estrogen and high progesterone. (2) 10 women receiving daily injections of follicle stimulating hormone (FSH) which allows for the development of multiple ovarian follicles for egg donation. This protocol was aimed at measuring the effects of greatly increased circulating estrogen levels (pregnancy levels) without high progesterone. The breast biopsy was obtained on the day of, or the day prior to, egg retrieval. (3) 37 post-menopausal women receiving menopausal estrogen therapy that also includes intra-vaginal micronized progesterone (E+P) or placebo (E alone). This protocol was aimed at measuring the effects of low levels of natural progesterone. Nineteen women on E+P were recruited and eighteen women on E alone.

Project 4

This project calls for the recruitment of 150 elective reduction mammoplasty, mastopexy or breast augmentation patients. The aim is to collect breast tissue from these women and conduct the same types of cellular, hormonal and genetic analyses as is being done in Project 3. In addition, cellular analyses on 100 tissue slides from previous reduction mammoplasties, and 100 autopsy breast tissue samples will be conducted. .

Task 1.   Months 1-48: Recruit 150 women undergoing elective reduction mammoplasty, mastopexy or breast augmentation to the protocol.

We have not been able to recruit any patients to the elective reduction protocol in the past 12 months. This is because the number of patients being seen by our plastic surgeons for this procedure has decreased drastically with the economy and other factors. In order to address this issue we have written three new protocols designed to obtain normal breast tissue; women undergoing elective mastopexies and augmentations and volunteers willing to undergo a breast biopsy (Project 3, Task 2d). We have revised the SOW accordingly and will be submitting the protocols to the DOD IRB.

Task 1a.   Months 1-36: Identify and conduct cellular assays on 100 tissue samples from previous reduction mammoplasties.

We have identified 100 tissue samples and have detailed questionnaire data on 73 of the cases. While continuing recruitment of the remaining 27, we have also amended the protocol to allow for medical record review to obtain information regarding hormone use, pregnancy history and other lifestyle factors in the event that we are unable to reach/locate the women. We expect to complete the cellular assays on these tissues within the next 6 months.

Task 1b. Months 23-54: Identify and conduct cellular assays on 100 autopsy breast tissue samples.

We have, in fact, obtained 230 such tissue samples. Initially we found that IHC on these samples was not satisfactory. With further work on antigen retrieval, we have now succeeded in obtaining completely satisfactory IHC results. These samples are now being prepared for both IHC and RNA extraction for use with DASL/NanoString. A secondary aim of this award is to better understand mammographic density as it is the strongest breast cancer risk factor. These samples are a very valuable resource in this regard.

These samples were collected by Dr. Sue Bartow while working at the Office of the New Mexico Medical Investigator between December 1978 and December 1983. She collected randomly selected breast tissue from autopsied women (Bartow et al., 1997). Samples of this tissue from women without breast cancer were used by Dr. Norman Boyd and colleagues to measure constituents of the tissue (Li et al., 2005). Specifically from tissue slices which had been X-rayed (Faxitron) by Dr. Bartow and the Faxitron density measured (Faxitron percent density; Faxitron %), Dr. Boyd and colleagues obtained slides and measured the areas of the slide occupied by tissue (total area, TA), by collagen (collagen area, CA) and by epithelial nuclear material (epithelial nuclear area, ENA). From these measurements they calculated collagen percent (CP = $100 \times$ CA/TA; Collagen %) and epithelial nuclear area percent (ENP = $100 \times$ ENA/TA; Epithelial Nuclear Area %) and showed that Collagen % was highly correlated with Faxitron %. Dr. Boyd and colleagues kindly provided this data to us to allow us to investigate more fully the relationship between Collagen % and Epithelial Nuclear Area % and how they relate to other personal data that Dr. Bartow had collected on the women in the study. Fig. 11 shows the very close relationship between Collagen % and Faxitron %. Mammographic (Faxitron) densities essentially represent the collagen content of the breast.
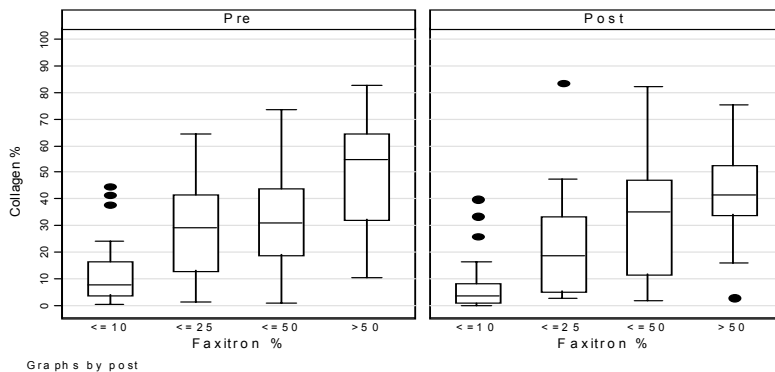

Figure 11. Relation of Collagen % to Faxitron % in premenopausal (Pre) and postmenopausal (Post) women (Figure 1 from Pike et al., in review).

17

We previously showed (Hawes et al., 2006) as part of this grant that a very high proportion of breast epithelial tissue is contained within dense collagen areas. Figure 12 shows the correlation of Epithelial Nuclear Area % and Collagen %, confirming the relationship we found previously. The relationship is clearly different in premenopausal compared to postmenopausal women. There is much less Epithelial Nuclear Area % per Collagen % in postmenopausal women than in premenopausal women. In postmenopausal women, there is a close to a proportional relationship between Epithelial Nuclear Area % and Collagen %. In premenopausal women there is more epithelium per unit collagen area at low collagen percentages.
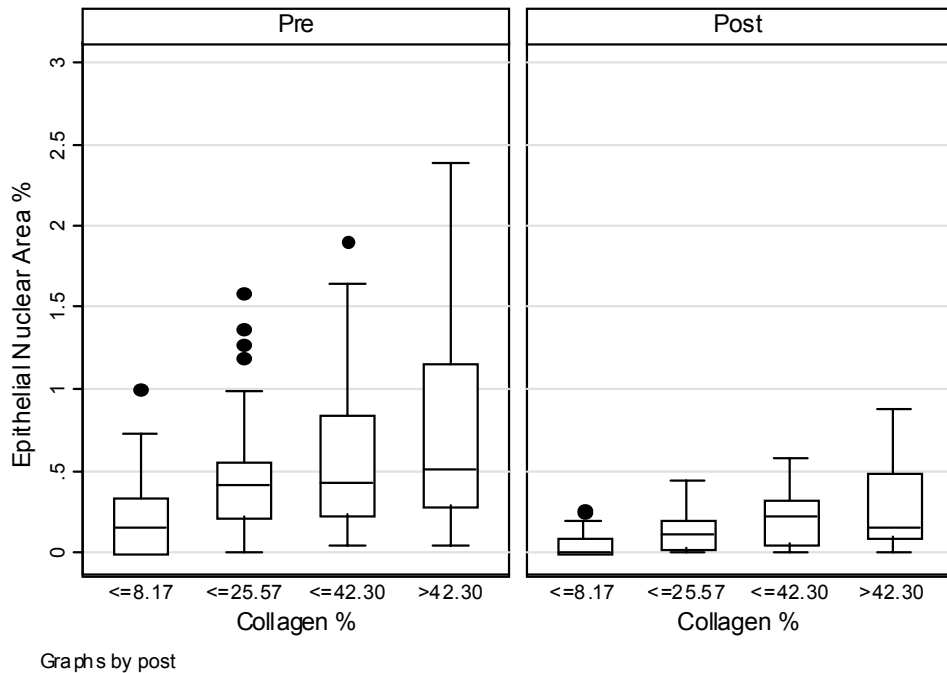

Graphs by post

Figure 12. Relation of Epithelial Nuclear Area % to Collagen % in premenopausal (Pre) and postmenopausal women.

The strongest 'environmental' factor influencing mammographic densities is parity. Mammographic densities are steadily reduced with each birth, as is long-term breast cancer risk. An important question to ask is whether the concentration of epithelium in collagen is affected by births. If the amount of breast epithelium is not affected by parity then this will increase with births due to the decrease in collagen (mammographic density) with births. Analysis suggests that as densities (collagen) decrease, epithelium decreases but to a smaller extent. This provides a fundamental insight into the mechanism of the protective effect of births against breast cancer, namely, births may decrease the tissue (epithelium) at risk. A manuscript describing these findings has been submitted for publication; our revised manuscript is being reviewed (Pike et al., submitted).

Task 2. Months 5-48: Assay tissue samples for hormonal and cellular markers to determine dense and non-dense tissue characteristics, and their association with glandular tissue proliferation.

We have assayed the tissue for a series of hormonal and cellular markers. To date, we have characterized ER expression, PR-A expression, PR-B expression, as well as quantified cell proliferation in the samples collected as part of Tasks 1 and 1a (Taylor et al., 2009).

Task 3.   Months 5-48: Assay blood samples for hormone levels.

We have provided the samples to the lab for hormone analysis.

Task 4.   Months 37-48: Conduct gene expression arrays on the dense and non-dense tissue samples to determine if the expression profiles differ.

As described above this work has proved difficult but we are conscientiously pursuing the possibility of conducting these assays with DASL/NanoString.

Task 5.   Months 13-60: Conduct data analysis to compare dense and non-dense tissue characteristics and prepare manuscripts as appropriate.

We are continuing to analyze the data we have collected; have one manuscript in review and another in preparation.

KEY RESEARCH ACCOMPLISHMENTS:

- Treatment of rats with hormonal chemoprevention regimens and determination of effective regimens.
- Evaluation of rat mammary gland morphology.
- Identification of genes expressed in a parity-specific manner in multiple rat strains resulting in a key publication (Blakely *et al.*, *Cancer Research,* 66:6421-6431, 2006; erratum in 67:844-846, 2007).
- Development and initiation of a protocol to allow us to evaluate the appropriateness of a progestin-based breast cancer chemopreventive approach.
- Development and initiation of a protocol to collect interview data, tissue specimens, and mammograms on women having elective reduction mammoplasties.
- Development of a protocol to allow us to evaluate breast cell proliferation in women receiving different progestin-dose oral contraceptives.
- Development of a protocol to allow us to evaluate breast cell proliferation in women receiving micronized progesterone versus placebo to determine the effect of exogenous progesterone on proliferation.
- Development of a protocol to allow us to evaluate the effects of high dose estrogen on breast tissue.
- Development of a protocol to allow us to collect breast tissue from women undergoing mastopexy procedures.
- Development of a protocol to allow us to collect breast tissue from women receiving a breast augmentation.
- Development of a protocol to allow us to collect breast tissue from healthy volunteers.
- Evaluation of tissue samples from reduction mammoplasties resulting in a seminal publication (Hawes *et al.*, *Breast Cancer Research,* 8:R24-29, 2006).
- Contact and interview 27 additional previous reduction mammoplasty subjects to obtain demographic, reproductive, and hormone use data.
- Identify remaining 43 previous reduction mammoplasty subjects to obtain demographic, reproductive and hormone use data.
- Staining and evaluation of ER-A, PR-A, and PR-B expression and cell proliferation in previous reduction mammoplasty samples and prospective reduction mammoplasty samples.
- Discovery of a sustaining decrease in PR-A after pregnancy as a potential marker of the protective effect of pregnancy on breast cancer risk (Taylor *et al.*, 2009; add citation).
- Development of methods for laser capture microscopy (LCM) to isolate relevant cell populations.
- Successful RNA extraction, quantitation and integrity evaluation from partially LCM dissected samples followed by quantitative gene expression measurement of both high and low abundance markers.
- A further key accomplishment is the development of a network of collaborators at USC and across the United States to further the work being funded by this grant.
    - At USC we continue to have lively bi-monthly meetings of our working group of investigators with expertise in endocrinology, gynecology, breast

cancer pathology, oncology, radiology, epidemiology and molecular biology/embryology who meet at least twice a month to review progress of the various projects and specific related tasks and to discuss any data generated from the studies and any new questions that may arise from our studies or published literature.

- o We continue to have fruitful collaborations with Dr. Sue Bartow for studies on breast specimens from autopsies performed in New Mexico. These are the same specimens utilized by Dr. Norman Boyd's group (Li *et al.*, *Cancer Epidemiol Biomarkers Prev,* 14:343-349, 2005) and we have collaborated and are continuing to collaborate with Dr. Boyd in analyzing these data further.

- Demonstration that low-dose and short-term hormone treatment of rats reduces mammary tumor susceptibility.
- Extensive attempts to recapitulate hormone and parity-induced protection against mammary tumorigenesis in mice.

REPORTABLE OUTCOMES:

1. Blakely CM, Stoddard AJ, Belka GK, Dugan KD, Notarfrancesco KL, Moody SE, D'Cruz CM, and Chodosh LA. Hormone-induced protection against mammary tumorigenesis is conserved in multiple rat strains and identifies a core gene expression signature induced by pregnancy. *Cancer Research*, 66:6421-6431, 2006; erratum in 67:844-846, 2007.
2. Hawes D, Downey S, Pearce CL, Bartow S, Wan P, Pike MC, Wu AH. Dense breast stromal tissue shows greatly increased concentration of breast epithelium but no increase in its proliferative activity. *Breast Cancer Res*, 8:R24-29, 2006.
3. Taylor D, Pearce CL, Hovanessian-Larsen L, Downey S, Spicer DV, Bartow S, Ling C, Pike MC, Wu AH, Hawes D. Progesterone and estrogen receptors in pregnant and premenopausal non-pregnant normal human breast. *Breast Cancer Res Treat,* 10 February 2009 published on line.

CONCLUSION:

Our finding that PR-A expression appears to be altered during and following pregnancy provides a potentially important insight into a marker for mimicking the protective effect of a pregnancy on breast cancer risk.

Our finding that breast epithelial tissue in women is overwhelmingly concentrated in mammographically dense areas of the breast (areas of high collagen concentration not seen in rodent breast) provides a deep insight into the reason for increased mammographic density being so closely associated with increased risk of breast cancer - women with increased mammographic density have more breast epithelium. The reason(s) for this relationship is at present unclear and is a focus of our current research. Breast densities are reduced in parous compared to nulliparous women, so that this endeavor ties in closely with our development of a chemoprevention regimen to mimic the protective effect of pregnancy. It may be that the genetic expression changes brought about by pregnancy (discussed above) are themselves responsible for the reduction in densities.

The development of new technology which reduces the amount and quality of RNA needed for expression studies will enable us to conduct large scale gene expression studies on the relevant breast cell populations over the next year. This will, we hope, provide further insight into the characteristics of the parous breast which ultimately provides protection against breast cancer. This work will be guided by the significant progress Projects 1 and 2 have made into identifying potential expression markers of the protective effects of pregnancy and hormone treatments against breast cancer.

REFERENCES:

1. Bartow SA, Mettler FA, Black WC. Correlations between radiographic patterns and morphology of the female breast. *Rad Patterns Morph*, 13:263-275, 1997.
2. Blakely CM, Stoddard AJ, Belka GK, Dugan KD, Notarfrancesco KL, Moody SE, D'Cruz CM, and Chodosh LA. Hormone-induced protection against mammary tumorigenesis is conserved in multiple rat strains and identifies a core gene expression signature induced by pregnancy. *Cancer Research*, 66:6421-6431, 2006; erratum in 67:844-846, 2007.
3. Hawes D, Downey S, Pearce CL, Bartow S, Wan P, Pike MC, Wu AH. Dense breast stromal tissue shows greatly increased concentration of breast epithelium but no increase in its proliferative activity. *Breast Cancer Res*, 8:R24-29, 2006.
4. Lee SA, Ross RK, Pike MC. An overview of menopausal oestrogen-progestin hormone therapy and breast cancer risk. *Brit J Cancer*, 92:2049-2058, 2005.
5. Li T, Sun L, Miller N, Nicklee T,Woo J,Hulse-Smith L,Tsao MS,Khokha R, Martin L, Boyd N. *Cancer Epidemiol Biomarkers Prev,* 14:343-349, 2005.

APPENDICES:

1. List of personnel
2. Blakely CM, Stoddard AJ, Belka GK, Dugan KD, Notarfrancesco KL, Moody SE, D'Cruz CM, and Chodosh LA. Hormone-induced protection against mammary tumorigenesis is conserved in multiple rat strains and identifies a core gene expression signature induced by pregnancy. *Cancer Research*, 66:6421-6431, 2006; erratum in 67:844-846, 2007.
3. Hawes D, Downey S, Pearce CL, Bartow S, Wan P, Pike MC, Wu AH. Dense breast stromal tissue shows greatly increased concentration of breast epithelium but no increase in its proliferative activity. *Breast Cancer Res*, 8:R24-29, 2006.
4. Taylor D, Pearce CL, Hovanessian-Larsen L, Downey S, Spicer DV, Bartow S, Ling C, Pike MC, Wu AH, Hawes D. Progesterone and estrogen receptors in pregnant and premenopausal non-pregnant normal human breast. *Breast Cancer Res Treat*, . 10 February 2009 published on line.

Personnel List 2008-2009

University of Southern California – Projects 3 & 4

Malcolm C. Pike
Anna H. Wu
C. Leigh Pearce
L. Hovannesian-Larsen
Debra Hawes
Michael F. Press
Sue Ellen Martin
Frank Stanczyk
Jonathan Buckley
Lilly Chang
Alex Trana
Angela Umali
Peggy Wan
Lillian Young
Serina Ovalle

University of Pennsylvania – Projects 1 & 2

Lewis H. Chodosh
Chien-Chung Chen
Celina D'Cruz
Congzhou Liu
Patrick Taulman
Jinling Wu
Dhruv Pant
Adanma Ezidinma

Hormone-Induced Protection against Mammary Tumorigenesis Is Conserved in Multiple Rat Strains and Identifies a Core Gene Expression Signature Induced by Pregnancy

Collin M. Blakely, Alexander J. Stoddard, George K. Belka, Katherine D. Dugan, Kathleen L. Notarfrancesco, Susan E. Moody, Celina M. D'Cruz, and Lewis A. Chodosh

Departments of Cancer Biology, Cell and Developmental Biology, and Medicine, and The Abramson Family Cancer Research Institute, University of Pennsylvania School of Medicine, Philadelphia, Pennsylvania

Abstract

Women who have their first child early in life have a substantially lower lifetime risk of breast cancer. The mechanism for this is unknown. Similar to humans, rats exhibit parity-induced protection against mammary tumorigenesis. To explore the basis for this phenomenon, we identified persistent pregnancy-induced changes in mammary gene expression that are tightly associated with protection against tumorigenesis in multiple inbred rat strains. Four inbred rat strains that exhibit marked differences in their intrinsic susceptibilities to carcinogen-induced mammary tumorigenesis were each shown to display significant protection against methylnitrosourea-induced mammary tumorigenesis following treatment with pregnancy levels of estradiol and progesterone. Microarray expression profiling of parous and nulliparous mammary tissue from these four strains yielded a common 70-gene signature. Examination of the genes constituting this signature implicated alterations in transforming growth factor-β signaling, the extracellular matrix, amphiregulin expression, and the growth hormone/insulin-like growth factor I axis in pregnancy-induced alterations in breast cancer risk. Notably, related molecular changes have been associated with decreased mammographic density, which itself is strongly associated with decreased breast cancer risk. Our findings show that hormone-induced protection against mammary tumorigenesis is widely conserved among divergent rat strains and define a gene expression signature that is tightly correlated with reduced mammary tumor susceptibility as a consequence of a normal developmental event. Given the conservation of this signature, these pathways may contribute to pregnancy-induced protection against breast cancer. (Cancer Res 2006; 66(12): 6421-31)

Introduction

Epidemiologic studies clearly show that a woman's risk of developing breast cancer is influenced by reproductive endocrine events (1). For example, early age at first full-term pregnancy, as well as increasing parity and duration of lactation, have each been shown to reduce breast cancer risk (2, 3). In particular, women who have their first child before the age of 20 have up to a 50% reduction in lifetime breast cancer risk compared with their nulliparous counterparts (2). Notably, the protective effects of an early full-term pregnancy have been observed in multiple ethnic groups and geographic locations, suggesting that parity-induced protection results from intrinsic biological changes in the breast rather than specific socioeconomic or environmental factors. At present, however, the biological mechanisms underlying this phenomenon are unknown.

Several models to explain the protective effects of parity have been proposed. For instance, parity has been hypothesized to induce the terminal differentiation of a subpopulation of mammary epithelial cells, thereby decreasing their susceptibility to oncogenesis (4). Related to this, parity has been suggested to induce changes in cell fate within the mammary gland, resulting in a population of mammary epithelial cells that are more resistant to oncogenic stimuli by virtue of decreased local growth factor expression and/or increased transforming growth factor (Tgf)-β3 and p53 activity (5, 6). Others have suggested that the process of involution that follows pregnancy and lactation acts to eliminate premalignant cells or cells that are particularly susceptible to oncogenic transformation (5). Conversely, parity-induced decreases in breast cancer susceptibility could also be due to persistent changes in circulating hormones or growth factors rather than local effects on the mammary gland (7). At present, however, only limited cellular or molecular evidence exists to support any of these models.

Similar to humans, both rats and mice exhibit parity-induced protection against mammary tumorigenesis. Administration of the chemical carcinogens, 7,12-dimethylbenzanthracene or methylnitrosourea, to nulliparous rats results in the development of hormone-dependent mammary adenocarcinomas that are histologically similar to human breast cancers (8). In outbred Sprague-Dawley, and inbred Lewis and Wistar-Furth rats, a full-term pregnancy either shortly before or after carcinogen exposure results in a high degree of protection against mammary carcinogenesis (7, 9, 10). Similarly, treatment of rats with pregnancy-related hormones, such as 17-β-estradiol (E) and progesterone (P), can mimic the protective effects of pregnancy in rat mammary carcinogenesis models (11, 12). This suggests that the mechanisms of parity-induced protection and estradiol and progesterone–induced protection may be similar. Using analogous approaches, Medina and colleagues have shown parity-induced as well as hormone-induced protection against 7,12-dimethylbenzanthracene–initiated carcinogenesis in mice (13, 14). As such, rodent models recapitulate the ability of reproductive endocrine events to modulate breast cancer risk as observed in humans. This, in turn, permits the mechanisms of parity-induced protection to be studied within defined genetic and reproductive contexts.

Previously, analyses of gene expression changes that occur in rodent models in response to parity, or hormonal treatments that mimic parity, have been used to suggest potential cellular and molecular mechanisms for pregnancy-induced protection against breast cancer (6, 15). Rosen and colleagues used subtractive hybridization analysis to identify genes in the mammary glands of Wistar-Furth rats that were persistently up-regulated 4 weeks posttreatment with estradiol and progesterone (15). Estradiol and progesterone treatment was found to increase the mRNA expression of a wide range of genes, including those involved in differentiation, cell growth, and chromatin remodeling. Similarly, we used microarray expression profiling to assess global gene expression changes induced by parity in the mammary glands of FVB mice (6). This analysis revealed parity-induced increases in epithelial differentiation markers, *Tgfb3* and its downstream targets, and cellular markers reflecting the influx of macrophages and lymphocytes into the parous gland. We also found that parity resulted in persistent decreases in the expression of a number of growth factor–encoding genes, including amphiregulin (*Areg*) and insulin-like growth factor (*Igf-I*). Together, these studies provided initial insights into cellular and molecular mechanisms that could contribute to parity-induced protection.

Notably, early first full-term pregnancy in humans primarily decreases the incidence of estrogen receptor (ER)-positive breast cancers (16). Because rats are more similar to humans than are mice with respect to the incidence of ER-positive mammary tumors (17), in the present study we used microarray expression profiling to identify persistent gene expression changes in the mammary glands of this rodent species to explore potential mechanisms of parity-induced protection. To date, a comprehensive analysis of parity-induced up-regulated and down-regulated gene expression changes in the rat has not been performed.

A major challenge posed by global gene expression surveys is the large number of differentially expressed genes that are typically identified, only a few of which may contribute causally to the phenomenon under study. Consequently, we considered approaches to identifying parity-induced changes in the rat mammary gland that would permit the resulting list of expressed genes to be narrowed to those most robustly associated with parity-induced protection against mammary tumorigenesis. Given the marked genetic and biological heterogeneity between different inbred rat strains, we reasoned that identifying expression changes that are conserved across multiple strains exhibiting hormone-induced protection against mammary tumorigenesis would facilitate the identification of a core set of genes associated with parity-induced protection against breast cancer.

To achieve this goal, we focused on gene expression changes that are conserved among different strains of rats that exhibit hormone-induced protection against mammary tumorigenesis. We first identified four genetically distinct inbred rat strains that exhibit hormone-induced protection against methylnitrosourea-induced mammary tumorigenesis independent of their inherent susceptibility to this carcinogen. We then used oligonucleotide microarrays to identify a core 70-gene expression signature that closely reflects parity-induced changes in the mammary gland that were conserved among each of these strains. The results of this analysis extend prior observations with respect to parity-induced changes in the growth hormone/Igf-I axis, identify novel parity-induced changes associated with the extracellular matrix (ECM), and implicate a core set of pathways in pregnancy-induced protection against breast cancer.

Materials and Methods

Animals and tissues. Lewis, Wistar-Furth, Fischer 344, and Copenhagen rats (Harlan, Indianapolis, IN) were housed under 12-hour light/12-hour dark cycles with access to food and water ad libitum. Animal care was performed according to institutional guidelines. To generate parous (G1P1) rats, 9-week-old females were mated and allowed to lactate for 21 days after parturition. After 28 days of postlactational involution, rats were sacrificed by carbon dioxide asphyxiation and the abdominal mammary glands were harvested and snap-frozen following lymph node removal, or whole-mounted and fixed in 4% paraformaldehyde. Whole-mounted glands were stained with carmine alum as previously described (6). For histologic analysis of whole mammary glands and tumors, paraffin-embedded tissues were sectioned and stained with H&E or Mason's trichrome as previously described (6). Tissues were harvested from age-matched nulliparous (G0P0) animals in an identical manner.

Carcinogen and hormone treatments. Twenty-five to 30 nulliparous female Lewis, Fischer 344, Wistar-Furth, and Copenhagen rats were weighed and treated at 7 weeks of age with methylnitrosourea (Sigma-Aldrich, St. Louis, MO) at a dose of 50 mg/kg by a single i.p. injection. At 9 weeks of age, animals from each strain were assigned to one of two groups and treated with hormone pellets (Innovative Research, Sarasota, FL) by s.c. implantation. Group 1 received pellets containing 35 mg of 17-β-estradiol + 35 mg of progesterone, whereas group 2 received pellets containing placebo. Pellets were removed after 21 days of treatment. No signs of toxicity were observed. The development of mammary tumors was assessed by weekly palpation. Animals were sacrificed at a predetermined tumor burden, or at 60 weeks postmethylnitrosourea. At sacrifice, all mammary glands were assessed for tumors, which were fixed in 4% paraformaldehyde and embedded in paraffin. Tumor samples from each strain were confirmed as carcinomas by histologic evaluation. Statistical differences in tumor-free survival between experimental groups were determined by log rank tests and by the generation of hazard ratios (HR) based on the slope of the survival curves using GraphPad Prism 4.0 software.

Microarray analysis. RNA was isolated from snap-frozen abdominal mammary glands by the guanidine thiocyanate/cesium chloride method as previously described (6). Ten micrograms of total RNA from individual Wistar-Furth (six G0P0 and five G1P1), Fischer 344 (eight G0P0 and six G1P1), and Copenhagen (six G0P0 and five G1P1) rats was used to generate cDNA and biotinylated cRNA as previously described (6). For Lewis rats, three G0P0 and three G1P1 samples were analyzed, each of which was comprised of 10 μg of pooled RNA from three animals. To permit the identification of epithelial as well as stromal gene expression changes, intact mammary glands (with lymph nodes removed) were used. Samples were hybridized to high-density oligonucleotide microarrays (RGU34A) containing ~8,800 probe sets representing ~4,700 genes and expressed sequence tags. Affymetrix comparative algorithms (MAS 5.0) and Chipstat were used to identify genes that were differentially expressed between nulliparous and parous samples (18). Robust Multichip Average signal values were generated using Bioconductor (19).

Genes were selected for further analysis whose expression changed significantly by the above analysis in three out of four strains. Significance was assessed by randomly generating eight lists equal in size to the up-regulated and down-regulated lists for each strain from the population of nonredundant genes called present on the chip in at least one sample (2,428 genes). One million random draw trials were performed to calculate a nominal *P* value for combined list length and to estimate the false discovery rate (FDR) using the median list size occurring by chance.

Hierarchical clustering was done using R statistical software[1] and as described (20). Mouse genes were identified using the Homologene database (National Center for Biotechnology Information).

Quantitative real-time PCR. Five micrograms of DNase-treated RNA were used to generate cDNA by standard methods. *Csn2, Mmp12, Tgfb3*,

---

[1] http://www.R-project.org.

Igfbp5, Areg, Igf-I, Ghr, Serpinh1, and *Sparc* were selected for confirmation by quantitative real-time PCR (QRT-PCR) using TaqMan assays (Applied Biosystems, Foster City, CA). *B2m* was used as a control (21, 22). Reactions were performed in duplicate in 384-well microtiter plates in an ABI Prism Sequence Detection System according to standard methods (Applied Biosystems). One-tailed *t* tests were performed to determine statistical significance using Prism 4.0 software.

Results

Hormone-induced protection in inbred rat strains. To determine whether hormone-induced protection against mammary tumorigenesis is a feature unique to carcinogen-sensitive strains, we compared the extent of protection induced by hormones in four different rat strains: Lewis, Wistar-Furth, Fischer 344, and Copenhagen. Two of these strains (Lewis and Wistar-Furth) have been reported to exhibit hormone-induced protection (9, 12). However, it has not been determined whether carcinogen-resistant strains of rats, such as Copenhagen (23), also exhibit protection. Female rats from each strain were treated with a single dose of methylnitrosourea at 7 weeks of age, followed by s.c. implantation of either placebo or hormone pellets (35 mg of estradiol + 35 mg of progesterone) at 9 weeks of age. Among the placebo-treated groups, Lewis rats exhibited the highest susceptibility to methylnitrosourea-induced mammary tumorigenesis with 100% penetrance and a median tumor latency of 13 weeks (Fig. 1*A*). Fischer 344 and Wistar-Furth rats displayed intermediate carcinogen sensitivity with latencies of 24 and 36 weeks, respectively. In contrast, Copenhagen rats exhibited a high degree of resistance to methylnitrosourea-induced mammary tumorigenesis with only 5 of 12 animals developing mammary tumors, with an average latency of 51 weeks.

Surprisingly, despite the wide variance in carcinogen sensitivity of nulliparous rats from these four strains, estradiol and progesterone treatment induced a significant ($P < 0.05$) degree of protection against mammary tumorigenesis in each strain (Fig. 1*B*). For example, whereas Lewis and Copenhagen strains differed markedly in their sensitivity to methylnitrosourea, they exhibited strikingly similar degrees of hormone-induced protection with HRs of 0.19 [95% confidence interval (CI), 0.05-0.40] and 0.16 (95% CI, 0.02-0.63), respectively. The Wistar-Furth (HR, 0.31; 95% CI, 0.09-0.90) and Fischer 344 (HR, 0.38; 95% CI, 0.10-0.71) strains exhibited lesser, but significant degrees of protection. These experiments show that hormone treatments that mimic pregnancy confer protection against mammary tumorigenesis in each strain irrespective of the intrinsic carcinogen susceptibility of nulliparous animals from that strain.

Morphologic changes induced by parity in the rat mammary gland. Parity-induced changes in breast cancer susceptibility have been reported to be accompanied by persistent changes in the structure of the mammary gland in humans, as well as in rats and mice (4, 6). Consistent with this, carmine-stained whole-mount analysis of nulliparous and parous mammary glands from each of the four rat strains revealed that the architecture of the parous mammary epithelial tree was more complex than that of age-matched nulliparous animals, with a higher degree of ductal side-branching (Fig. 1*C*). These effects were observed in each of the four strains analyzed, suggesting that changes in the structural and cellular composition of the mammary gland may occur as a consequence of parity.

Microarray analysis of parity-induced changes in the rat mammary gland. The similar morphologic changes induced by parity suggested that the hormone-induced protection against mammary tumorigenesis that we observed in different rat strains might be accompanied by common molecular alterations. To identify these changes, we first performed oligonucleotide microarray expression profiling on pooled samples from nulliparous and parous Lewis rats. Genes whose expression changes were considered to be statistically significant using established algorithms, and whose expression changed by at least 1.2-fold as a result of parity, were selected for further analysis (18). This combined analytic approach has previously been shown to be capable of identifying differentially expressed genes with high sensitivity and specificity (18). Gene expression analysis performed in this manner identified 75 up-regulated and 148 down-regulated genes in parous compared with nulliparous mammary glands. Examination of this list of differentially expressed genes confirmed our previous findings in mice that parity results in the persistent up-regulation of *Tgfb3*, as well as differentiation and immune markers, as well as the persistent down-regulation of growth factor encoding genes, such as *Areg* and *Igf-I* (ref. 6; data not shown).

To narrow the list of candidate genes whose regulation might contribute to the protected state associated with parity, we attempted to identify parity-induced gene expression changes that were conserved across multiple rat strains. To this end, total RNA was isolated from the mammary glands of nulliparous and parous Wistar-Furth, Fischer 344, and Copenhagen rats, and analyzed on RGU34A arrays in a manner analogous to that employed for Lewis rats. This led to the identification of 68, 64, and 92 parity up-regulated genes and 132, 209, and 149 parity down-regulated genes in Wistar-Furth, Fischer 344, and Copenhagen rats, respectively.

Unsupervised hierarchical clustering performed using the expression profiles of 1,954 globally varying genes across the nulliparous and parous data sets representing the four rat strains revealed that samples clustered primarily based on strain without regard to parity status (Fig. 2*A*). This suggested that the principal source of global variation in gene expression across these data sets was due to genetic differences between strains rather than reproductive history. This observation suggested that determining which parity-induced gene expression changes were conserved among these highly divergent rat strains could represent a powerful approach to defining a parity-related gene expression signature correlated with hormone-induced protection against mammary tumorigenesis.

To identify parity-induced gene expression changes that were conserved across strains, we selected genes that exhibited ≥1.2-fold change in at least three of the four strains analyzed. This led to the identification of 24 up-regulated (Table 1) and 46 down-regulated genes (Table 2). Based on the number of parity-induced gene expression changes observed for each strain, an overlap of this size is highly unlikely by chance (up-regulated: $P < 1 \times 10^{-6}$, FDR < 1%; down-regulated: $P < 1 \times 10^{-6}$, FDR = 4%). As such, this approach led to the identification of 70 genes whose expression is persistently altered by parity across multiple strains of rats that exhibit hormone-induced protection against mammary tumorigenesis.

A gene expression signature distinguishes parous and nulliparous rats and mice. To confirm the validity of the 70-gene parity-related expression signature derived from the above studies, we performed oligonucleotide microarray analysis on samples from nulliparous and parous Lewis rats that were generated independently from those used to derive this signature. Hierarchical clustering analysis of these independent samples using the 70-gene signature revealed that the expression profiles of these genes were sufficient to accurately distinguish parous from nulliparous Lewis rat samples in a blinded manner (Fig. 2*B*).

To determine whether this parity-related signature could distinguish between nulliparous and parous mammary glands from multiple strains of rats, Lewis, Wistar-Furth, Fischer 344, and Copenhagen microarray data sets were clustered in an unsupervised manner based solely on the expression of the 70 genes comprising the parity signature (Fig. 2C). In each of the four rat strains examined, the 70-gene signature was sufficient

to distinguish parous from nulliparous rats (Fig. 2C). Thus, this signature reflects parity-induced gene expression changes that are highly conserved among four genetically divergent rat strains.

Early full-term pregnancy has been reported to result in protection against mammary tumorigenesis in mice, as it does in humans and rats (13). Accordingly, we mapped the 70 genes
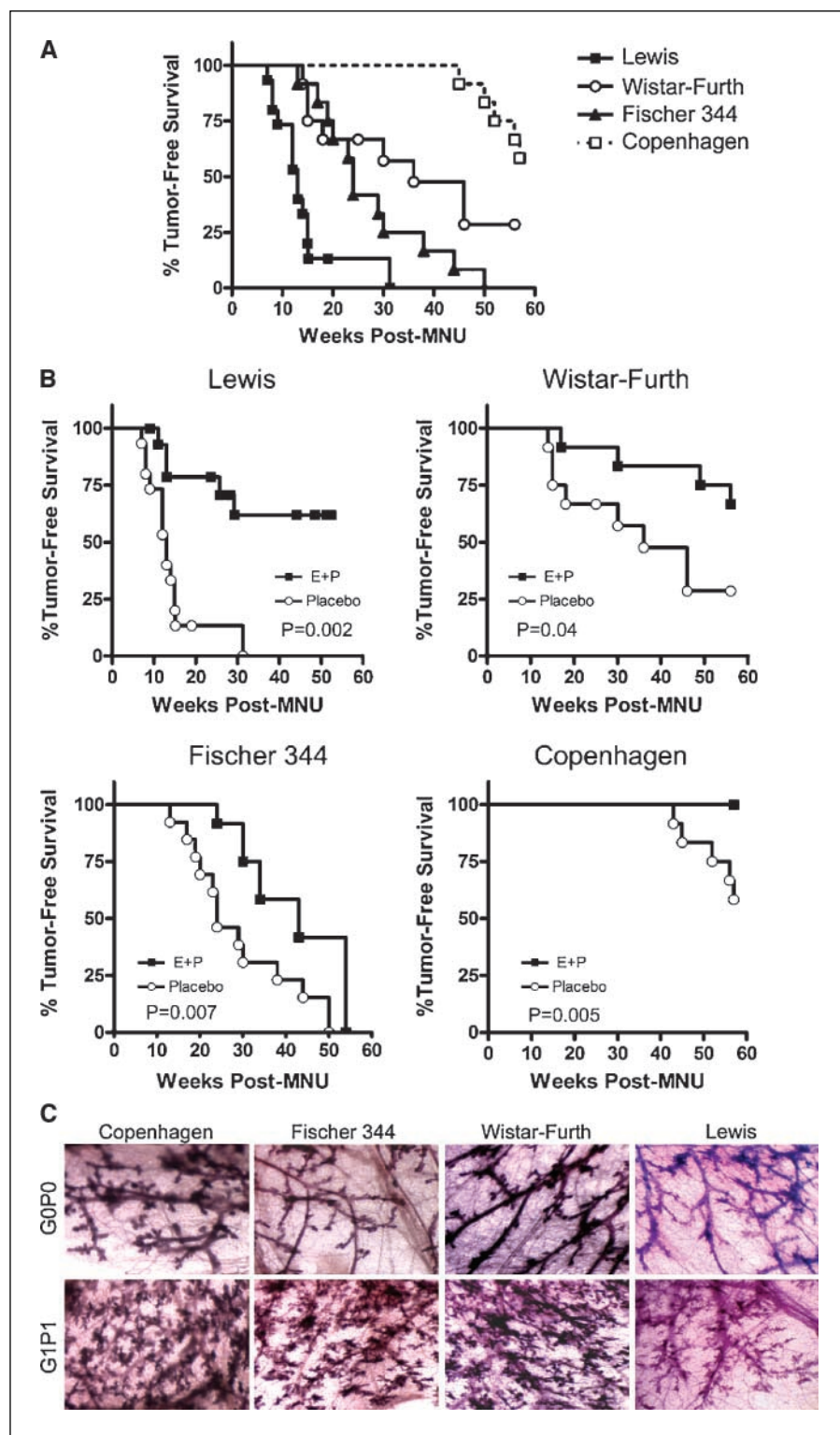

Figure 1. Hormone-induced protection against mammary tumorigenesis is conserved among multiple rat strains. *A,* Kaplan-Meier curves plotting the time to the formation of a first mammary tumor in placebo-treated groups for Lewis (*n* = 15), Wistar-Furth (*n* = 12), Fischer 344 (*n* = 13), and Copenhagen (*n* = 12) rats treated with methylnitrosourea (*MNU*) at 7 weeks of age. Significant differences in tumor incidence were identified between Lewis and Wistar-Furth (*P* = 0.0003), Lewis and Fischer 344 (*P* = 0.0005), Lewis and Copenhagen (*P* = 0.0001), Wistar-Furth and Copenhagen (*P* = 0.024), and Fischer 344 and Copenhagen (*P* = 0.0001) as determined by a log rank test. Wistar-Furth and Fischer 344 were not significantly different (*P* = 0.14). *B,* mammary tumor incidence for placebo and estradiol and progesterone–treated rats is plotted for each strain. Cohort sizes for estradiol and progesterone–treated animals were: Lewis (*n* = 16), Wistar-Furth (*n* = 12), Fischer 344 (*n* = 12), and Copenhagen (*n* = 12). Each strain exhibited significantly decreased tumor incidence in estradiol and progesterone–treated compared with placebo-treated cohorts. *C,* carmine-stained whole mounts of abdominal mammary glands from nulliparous (G0P0) and parous (G1P1) rats from each strain (original magnification, ×50). Samples are representative of three animals per group.
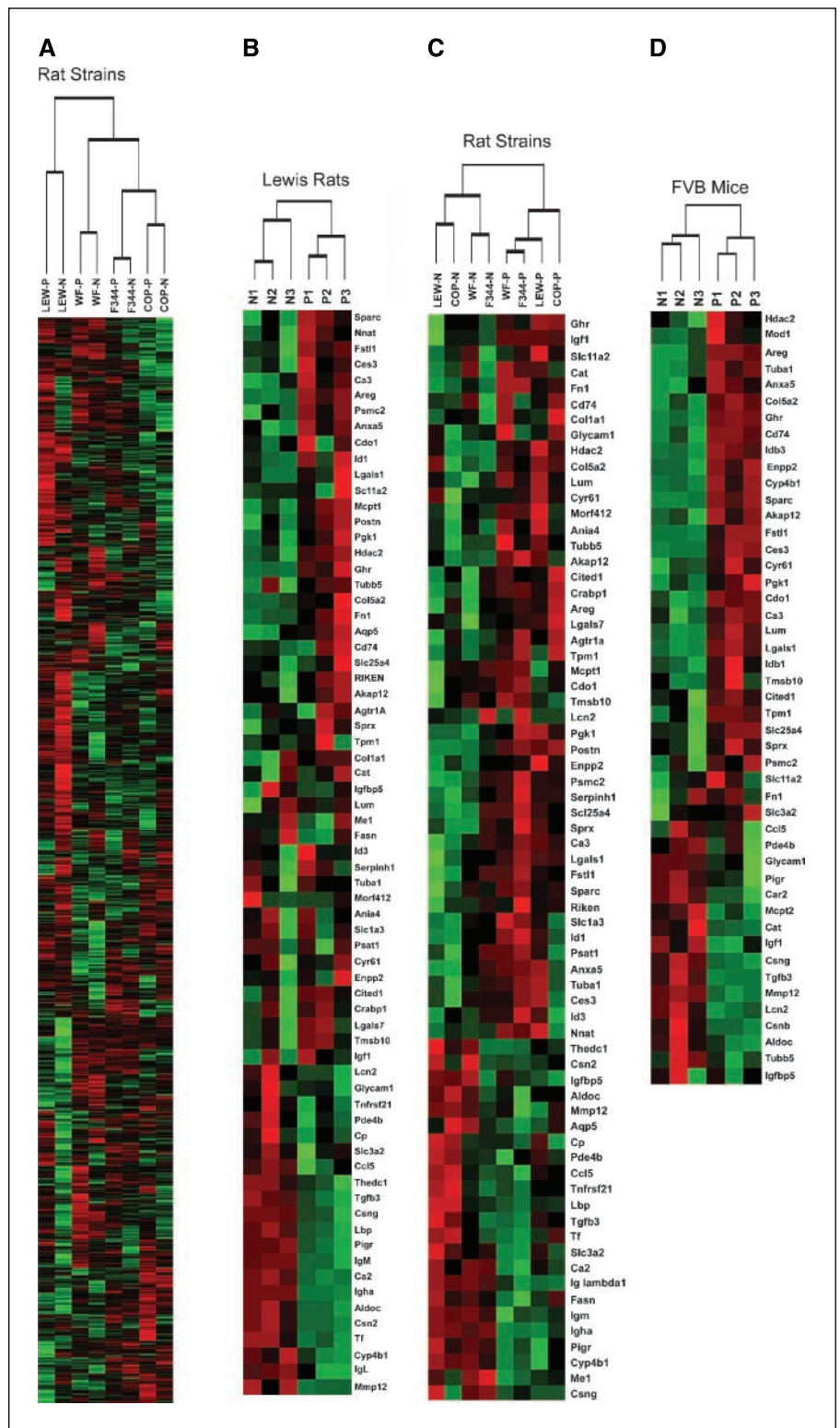
Figure 2. A parity-related gene expression signature distinguishes between nulliparous and parous rats and mice. Unsupervised hierarchical clustering analysis. Nulliparous (*N*), parous (*P*), Lewis (*LEW*), Fischer 344 (*F344*), Wistar-Furth (*WF*), and Copenhagen (*COP*). *A,* nulliparous and parous samples from each strain were clustered based on the median expression values of ~1,900 genes exhibiting global variation in gene expression across the data sets. *B,* six independent Lewis samples [three nulliparous (N1-N3) and three parous (P1-P3)] were clustered based solely on the expression of genes in the 70-gene parity signature. *C,* clustering analysis based solely on the expression of the 70-gene parity signature was performed on nulliparous and parous samples from Lewis, Wistar-Furth, Fischer, and Copenhagen rats. *D,* the 70-gene rat parity signature was mapped to the mouse genome using Homologene, yielding 47 mouse genes. Six FVB mouse samples [three nulliparous (N1-N3) and three parous (P1-P3)] were clustered based on the expression profiles of these 47 genes.

constituting the rat parity signature to the mouse genome, and assessed their expression profiles in nulliparous and parous FVB mouse mammary samples. Of the 70 genes that were mapped, 47 were represented on Affymetrix MGU74Av2 microarrays. These 47 genes were sufficient to distinguish nulliparous from parous samples in a blinded manner (Fig. 2*D*). Thus, a parity-related gene

expression signature generated in the rat is able to predict reproductive history in the mouse, suggesting that the persistent molecular alterations that occur in response to parity are conserved across rodent species.

Among the 70 genes that we identified as being consistently regulated by parity, at least five categories were evident.

Table 1. Genes up-regulated in parous rats

Gene name	Symbol	Gene ID	Function	Category	Fold-change G1P1 versus G0P0				
					Lewis	WF	F344	Cop	Median
Immunoglobulin heavy chain	*Igha*	314487	Immunoglobulin	Immune	39.4	25.4	4.5	6.9	25.4
Casein β	*Csn2*	29173	Milk protein	Differentiation	8.0	5.2	1.9	1.5	5.2
IgM light chain		287965	Immunoglobulin	Immune	2.5	3.8	1.8	1.6	2.5
Matrix metalloproteinase 12	*Mmp12*	117033	Proteolysis	ECM/Immune	2.6	1.4	2.0	1.3	2.0
Casein γ	*Csng*	114595	Milk protein	Differentiation	3.1	1.9	1.2	0.9	1.9
Fatty acid synthase	*Fasn*	50671	Fatty acid biosynthesis	Metabolism/ differentiation	2.0	1.6	1.7	0.9	1.7
Cytochrome P450, family 4, subfamily b,1	*Cyp4b1*	24307	Monooxygenase activity	Metabolism	1.6	1.5	1.2	1.2	1.5
Carbonic anhydrase 2	*Ca2*	54231	Carbon dioxide hydration	Metabolism	1.5	1.5	1.4	1.1	1.5
Ig lambda-1 chain C region		363828	Immunoglobulin	Immune	1.5	1.4	1.4	1.3	1.4
Malic enzyme 1	*Me1*	24552	Pyruvate synthesis	Metabolism	1.3	1.4	1.4	1.1	1.4
Insulin-like growth factor binding protein 5	*Igfbp5*	25285	Igf-I-binding	Growth factor/ ECM	2.4	1.4	0.9	2.7	1.4
Lipopolysaccharide binding protein	*Lbp*	29469	Antibacterial	Immune	2.1	1.3	1.4	2.0	1.4
Polymeric immunoglobulin receptor	*Pigr*	25046	Trancytosis	Immune	1.7	1.4	1.2	1.1	1.4
Transforming growth factor, β3	*Tgfb3*	25717	Cell growth/ proliferation	Tgf-β	1.5	1.3	1.2	1.4	1.3
Aquaporin 5	*Aqp5*	25241	Water transport	Transporter	1.3	1.7	1.2	1.5	1.3
Phosphodiesterase 4B	*Pde4b*	24626	Cyclic AMP phoshodiesterase	Signal transduction	1.3	1.4	1.0	1.4	1.3
Thioesterase domain containing 1	*Thedc1*	64669	Fatty acid biosynthesis	Metabolism/ differentiation	1.9	1.2	1.3	1.5	1.3
Transferrin	*Tf*	24825	Iron transport	Transport/ differentiation	1.4	1.2	1.3	1.5	1.3
Ceruloplasmin	*Cp*	24268	Copper transport	Transport/ differentiation	1.3	1.0	1.2	2.2	1.2
Similar to death receptor 6	*Tnfrsf21*	316256	Apoptosis	Signal transduction	1.3	1.0	1.2	1.3	1.2
Aldolase C, fructose-biphosphate	*Aldoc*	24191	Fructose metabolism	Metabolism	1.2	1.2	1.1	1.3	1.2
Lipocalin 2	*Lcn2*	170496	Iron binding/antibacterial	Immune	1.3	1.1	1.2	1.4	1.2
Solute carrier family 3, member 2	*Slc3a2*	50567	Amino acid transporter	Transporter	1.2	1.1	1.2	1.3	1.2

NOTE: Genes identified as up-regulated by at least 1.2-fold in three out of four rat strains as a result of parity are reported from the highest to lowest median fold change. Gene names and symbols are reported based on the Rat Genome Database, and Gene ID according to Entrez Gene. Gene functions and categories are based on Gene Ontology.

Abbreviations: WF, Wistar-Furth; F344, Fischer 344; Cop, Copenhagen.

These included the previously identified differentiation, immune, Tgf-β, and growth factor categories (6), as well as an additional category of genes that are involved in ECM structure and function (Tables 1 and 2). We previously showed that clustering based on genes in each of the first four categories was sufficient to distinguish between nulliparous and parous rats (6). In an analogous manner, we tested whether unsupervised clustering based solely on ECM-related genes would be sufficient to differentiate between nulliparous and parous rat or mouse samples. In each case, ECM-related gene expression patterns alone were sufficient to distinguish between nulliparous and parous mammary samples from the four different rat strains (Fig. 3*A*), from independent mammary samples derived from nulliparous and parous Lewis rats (Fig. 3*B*), and from mammary samples derived from FVB mice (Fig. 3*C*). This indicates that differential expression of a subset of genes involved in ECM structure and function represents a conserved feature of parity-induced changes in the rodent mammary gland.

Parity up-regulates *Tgfb3* and expression of differentiation and immune markers. Our previous analysis of parity-induced gene expression changes in FVB mice was consistent with the parity-induced up-regulation of Tgf-β3 activity. Similarly, in the current study, we found that *Tgfb3* expression was up-regulated by parity in each of the four rat strains examined (Table 1). This finding was confirmed by QRT-PCR

Table 2. Genes down-regulated in parous rats

Gene name	Symbol	Gene ID	Function	Category	Fold-change G1P1 versus G0P0				
					Lewis	WF	F344	Cop	Median
Periostin	*Postn*	361945	Transcription factor	Differentiation	1.9	2.1	1.8	2.2	2.0
Amphiregulin	*Areg*	29183	Epidermal growth factor receptor ligand	Growth factor	3.5	2.1	1.7	1.9	2.0
Cellular retinoic acid binding protein I	*Crabp1*	25061	Retinoic acid receptor signaling	Signal transduction	1.8	2.1	1.3	1.5	1.7
Insulin-like growth factor 1	*Igf-I*	24482	Cell proliferation/ survival	Growth factor	1.7	1.2	1.5	1.5	1.5
Fibronectin 1	*Fn1*	25661	Integrin signaling	ECM	1.4	1.3	1.5	1.6	1.5
A kinase (PRKA) anchor protein (gravin) 12	*Akap12*	83425	Scaffolding protein	Signal transduction	1.2	1.6	1.6	1.3	1.4
Neuronatin	*Nnat*	94270	Protein transport		2.0	1.4	1.5	0.9	1.4
Glycosylation dependent cell adhesion molecule 1	*Glycam1*	25258	Selectin ligand	Differentiation	0.5	2.2	1.2	1.7	1.4
Secreted acidic cysteine rich glycoprotein	*Sparc*	24791	ECM Formation	ECM	1.6	1.1	1.4	1.4	1.4
Ectonucleotide pyrophosphatase/ phosphodiesterase 2	*Enpp2*	84050	Lysophospholipase	Cell motility	2.1	1.4	1.4	1.0	1.4
Lectin, galactose binding, soluble 1	*Lgals1*	56646	Integrin signaling	ECM	1.5	1.2	1.4	1.4	1.4
Inhibitor of DNA binding 1, helix-loop-helix protein	*Id1*	25261	Transcriptional repression	Tgf-β	1.4	1.4	1.4	1.1	1.4
Follistatin-like 1	*Fstl1*	79210			1.5	1.7	1.2	1.2	1.4
Phosphoserine aminotransferase 1	*Psat1*	293820	Serine biosynthesis	Metabolism	1.4	1.2	1.5	1.3	1.4
Lumican	*Lum*	81682	Proteoglycan	ECM	1.3	1.5	1.1	1.4	1.3
Melanocyte-specific gene 1 protein	*Cited1*	64466	Transcription factor	Signal transduction	1.4	1.9	1.2	1.3	1.3
Serine proteinase inhibitor, clade H, member 1	*Serpinh1*	29345	Procollagen binding	ECM	1.4	1.3	1.3	1.4	1.3
Sushi-repeat-containing protein	*Sprx*	64316			1.3	1.3	1.3	1.5	1.3
Carboxylesterase 3	*Ces3*	113902	Fatty acid metabolism	Metabolism	1.8	1.1	1.3	1.4	1.3
Cysteine rich protein 61	*Cyr61*	83476	Integrin signaling	ECM	1.1	1.3	1.3	1.6	1.3
Solute carrier family 1, member 3	*Slc1a3*	29483	Amino acid transporter	Transporter	1.4	1.3	1.3	1.1	1.3
Similar to RIKEN cDNA 6330406I15	*RDG1307396*	360757			1.6	1.2	1.3	1.3	1.3
Catalase	*Cat*	24248	Hydrogen peroxide reductase	ROS	1.7	1.0	1.4	1.2	1.3
Tropomyosin 1, α	*Tpm1*	24851	Actin binding		1.1	1.3	1.3	1.3	1.3
Activity and neurotransmitter-induced early gene protein 4	*Ania4*	360341	CAM kinase	Kinase	1.5	1.2	1.2	1.3	1.3
Solute carrier family 11, member 2	*Slc11a2*	25715	Divalent metal ion transporter	Transporter	1.4	1.0	1.3	1.2	1.3
Inhibitor of DNA binding 3, helix-loop-helix protein	*Id3*	25585	Transcriptional repression	Tgf-β	1.5	1.2	1.3	0.9	1.3
Solute carrier family 25 member 4	*Slc25a4*	85333	Nucleotide translocator	Transporter	1.3	1.3	1.2	1.3	1.3
Growth hormone receptor	*Ghr*	25235	Growth hormone signaling	Growth factor	2.1	1.1	1.2	1.3	1.3
Phosphoglycerate kinase 1	*Pgk1*	24644	Phosphoprotein glycolysis	Metabolism	1.6	1.2	1.3	1.2	1.3

(*Continued on the following page*)

Table 2. Genes down-regulated in parous rats (Cont'd)

Gene name	Symbol	Gene ID	Function	Category	Fold-change G1P1 versus G0P0				
					Lewis	WF	F344	Cop	Median
Cytosolic cysteine dioxygenase 1	*Cdo1*	81718	Cysteine metabolism	Metabolism	1.5	1.2	1.2	1.3	1.3
Mast cell protease 1	*Mcpt1*	29265	Proteolysis	ECM	1.6	1.3	1.2	1.2	1.2
Collagen, type V, α2	*Col5a2*	85250	ECM structural protein	ECM	1.0	1.2	1.3	1.5	1.2
Carbonic anhydrase 3	*Ca3*	54232	Carbon metabolism	Metabolism	1.8	1.2	1.1	1.3	1.2
Tubulin, α1	*Tuba1*	64158	Microtubule component	Cell structure	1.5	1.2	1.2	1.2	1.2
Angiotensin II receptor, type 1	*Agtr1A*	24180	Angiotensin receptor	Signal transduction	1.3	1.2	1.2	1.3	1.2
Collagen, type 1, α 1	*Col1a1*	29393	ECM structural protein	ECM	1.1	1.2	1.2	1.8	1.2
Annexin A5	*Anxa5*	25673	Calcium ion binding		1.6	1.2	1.2	1.2	1.2
Thymosin, β10	*Tmsb10*	50665	Actin binding		1.3	1.2	1.2	1.0	1.2
Tubulin, β5	*Tubb5*	29214	Microtubule component	Cell structure	1.1	1.3	1.2	1.2	1.2
Histone deacetylase 2	*Hdac2*	84577	Chromatin rearrangement		1.2	1.2	1.3	1.1	1.2
Lectin, galactose binding, soluble 7	*Lgals7*	29518	Galactose binding		1.1	1.8	1.2	1.2	1.2
CD74 antigen	*Cd74*	25599		Immune	1.2	1.2	1.0	1.3	1.2
Proteasome 26S subunit, ATPase 2	*Psmc2*	25581	Protein degradation		1.3	1.1	1.2	1.1	1.2
MORF-related gene X	*Morf412*	317413			1.4	1.2	1.1	1.2	1.2

NOTE: Genes identified as down-regulated by at least 1.2-fold in three out of four rat strains as a result of parity are reported from the highest to lowest median fold change. Gene names and symbols are reported based on the Rat Genome Database, and Gene ID according to Entrez Gene. Gene functions and categories are based on Gene Ontology.

Abbreviations: WF, Wistar-Furth; F344, Fischer 344; Cop, Copenhagen.

analysis of independent parous and nulliparous Lewis rat samples (Fig. 4*A*).

Also consistent with our prior observations, parity resulted in a persistent increase in the expression of genes involved in mammary differentiation, including the milk proteins β-casein and γ-casein, and the metal ion transporters ceruloplasmin and tranferrin (ref. 6; Table 1; Fig. 4*A*).

As we have previously shown in the mouse, the 70-gene rat parity-related gene expression signature reflected the increased presence of immune cells in the parous mammary gland. In particular, increased expression of multiple immunoglobulin heavy and light chain genes in the parous gland suggested an increase in the population of plasma cells, whereas up-regulation of *Mmp12* and *Tnfrsf21* was consistent with increased numbers of macrophages and T cells (Table 1; Fig. 4*A*). Similarly, increased antibacterial and antiviral activity was suggested by the up-regulation of *Lbp, Lcn2*, and *Ccl5* (refs. 24–26; Table 1).

Parity results in down-regulation of amphiregulin and the growth hormone/Igf-I axis. Previous gene expression profiling of mouse mammary development revealed that parity results in a persistent decrease in the expression of several growth factor–encoding genes, including *Areg* and *Igf-I* (6). The present study confirmed that decreased expression of *Areg* and *Igf-I* are consistent features of the parous state in rats (Table 2; Fig. 4*B*). Additional evidence supporting parity-induced down-regulation of the growth hormone/Igf-I axis in the mammary glands of multiple rat strains was suggested by a decrease in growth hormone receptor (*Ghr*) expression (Table 2; Fig. 4*B*) as well as an increase in

Igfbp5 expression (Table 1; Fig. 4*A*), which functions to sequester local Igf-I in the ECM (27).

Parity regulates ECM gene expression. Mammary epithelial-ECM interactions play an important role in both normal mammary gland development and tumorigenesis (28). Moreover, persistent changes in the structure and function of the ECM have been shown in the mammary glands of parous rats (29). In the present study, microarray expression profiling suggested that a principal effect of parity in the rodent mammary gland is alteration of ECM gene expression. Thirteen of the 70 genes constituting the parity signature encode ECM structural components or proteins that regulate ECM formation or signaling (Tables 1 and 2). Notably, the majority of ECM-related gene expression changes induced by parity represented decreases in expression, including the ECM structural components, fibronectin 1, lumican, and collagen type I and collagen type V (Table 2). Parity-induced decreases in the expression of genes that regulate ECM formation or cellular interactions were also observed, including, *Sparc, Lgals1, Lgals7, Serpinh1, Cyr61*, and *Mcpt1* (Table 2; Fig. 4*B*).

To determine whether these parity-induced ECM-related gene expression changes were accompanied by differences in ECM structure, we stained histologic sections with Mason's trichrome to evaluate total collagen content. Although proximal epithelial structures seemed similar with respect to periductal trichrome staining (data not shown), a significant decrease in the extent of trichrome staining surrounding distal ducts was observed in the parous gland (Fig. 4*C*). These results provide further evidence that parity results in structural changes in the ECM.

Discussion

Women who have their first child early in life have a substantially reduced lifetime risk of breast cancer, an effect that is largely restricted to ER-positive tumors. Similar to humans, rats frequently develop ER-positive breast cancers and exhibit parity-induced protection against mammary tumorigenesis. In the current study, we set out to identify persistent parity-induced changes in gene expression that are conserved among multiple rat strains that exhibit hormone-induced protection against mammary tumorigenesis. We found that four genetically diverse inbred rat strains exhibit hormone-induced protection against mammary tumorigenesis and share a 70-gene pregnancy-induced expression signature. Our findings constitute the first global survey of parity-induced changes in gene expression in the rat—which represents the principal model for studying this phenomenon—as well as the first study to show conservation of parity-induced gene expression changes in multiple inbred rat strains that exhibit hormone-induced protection. Beyond suggesting that parity-induced protection is as robust and widely conserved a phenomenon in rats as it is in humans, our findings provide new insights into potential mechanisms by which early first-full term pregnancy decreases breast cancer risk.

These current studies extend our previous observations that parity results in persistently increased mammary expression of *Tgfb3* to include multiple additional strains of rats. Notably, loss of Tgf-β signaling in stromal fibroblasts promotes the growth and invasion of mammary carcinomas (30). Tgf-β may also have direct effects on mammary epithelial cells, resulting in the inhibition of mammary tumorigenesis (31). The sum of these effects is predicted to decrease the susceptibility of the parous gland to oncogenic transformation.

One of the most consistent and robust parity-induced changes in gene expression that we have observed in the rodent mammary gland is down-regulation of the epidermal growth factor receptor ligand, *Areg*. AREG is overexpressed in a high proportion of human breast cancers and correlates with large tumor size and nodal involvement (32). Studies in genetically engineered mice and mammary epithelial cell lines suggest an important role for AREG in driving mammary epithelial proliferation, whereas recent evidence indicates that this growth factor may alter the ECM by the regulation of protease expression and secretion, including matrix metalloproteinase-2, matrix metalloproteinase-9, urokinase-type plasminogen activator, and plasminogen activator inhibitor-1 (33). Thus, parity-mediated down-regulation of *Areg* may not only inhibit epithelial proliferation, but may also hinder the invasive abilities of transformed cells in the mammary gland.

In addition to the down-regulation of *Areg*, we have confirmed that parity also results in the persistent down-regulation of *Igf-I*. Notably, a strong positive correlation exists between serum IGF-I levels and breast cancer risk in premenopausal women (34). Local and serum levels of IGF-I are regulated by growth hormone through its interaction with growth hormone receptor (35). Additional findings indicate that parity results in a persistent decrease in circulating growth hormone levels in rats (7); moreover, treatment of parous rats with Igf-I results in an increase in carcinogen-induced mammary tumorigenesis to levels similar to those observed in nulliparous controls (36). Consistent with this, spontaneous dwarf rats, which lack functional growth hormone, are highly resistant to carcinogen-induced mammary tumorigenesis (37).

Additional evidence for down-regulation of the growth hormone/Igf-I axis within the parous mammary gland was suggested in the present study by increases in *Igfbp5* expression and decreases in *Ghr* expression. As such, our findings suggest that—in addition to reducing circulating levels of growth hormone—parity may modulate local expression and activity of Igf-I within the mammary gland. Whereas Igf-I acts directly on mammary epithelial cells to promote proliferation and inhibit apoptosis (38), Igf-I in the mammary gland is likely produced in the stromal compartment in response to Ghr signaling (39). Local regulation of Igf-I activity also occurs through interactions with Igf-I binding proteins, such as Igfbp5, which binds and sequesters Igf-I in the ECM (40). As such, parity-induced down-regulation of Ghr and Igf-I expression in the mammary gland, coupled with up-regulation of Igfbp5 expression, would be predicted to result in decreased Igf-I activity. This represents a

Figure 3. ECM gene expression distinguishes between nulliparous and parous rats and mice. Unsupervised hierarchical clustering analysis. *A,* a subset of parity-regulated genes involved in ECM structure and regulation was used to cluster nulliparous and parous mammary samples from Lewis (*LEW*), Wistar-Furth (*WF*), Fischer (*F344*), and Copenhagen (*COP*) rats. *B,* six independent Lewis samples [three nulliparous (N1-N3) and three parous (P1-P3) samples] were clustered based on the expression of ECM-related genes. *C,* six FVB mouse samples [three nulliparous (N1-N3) and three parous (P1-P3)] were clustered based on the expression of ECM-related genes identified in the rat parity signature that were mapped to the mouse genome.
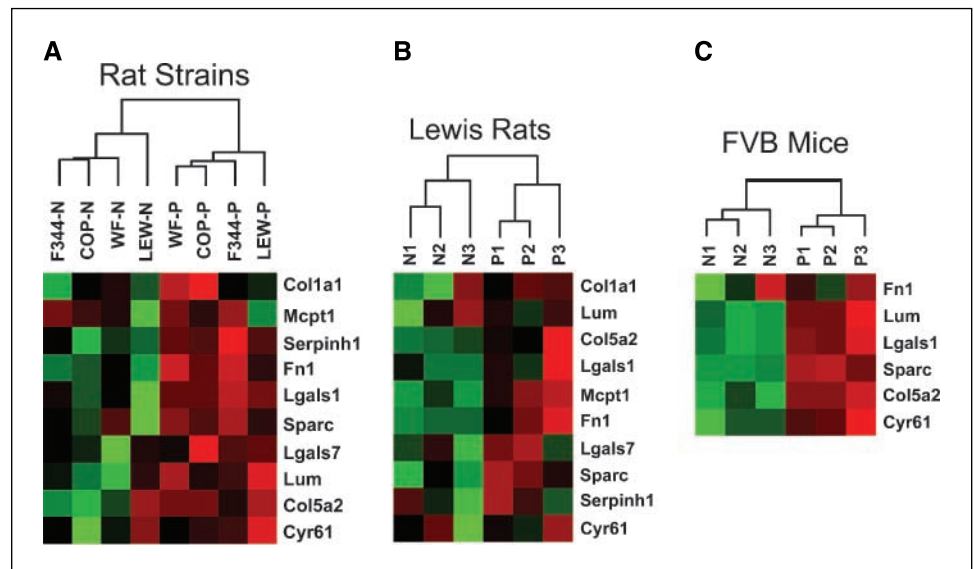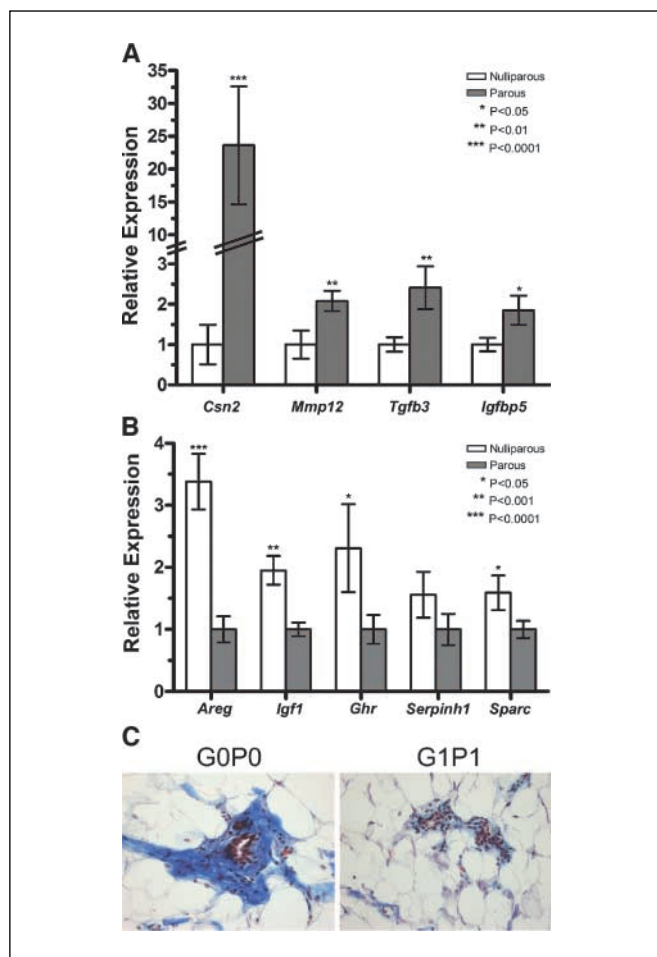
Figure 4. Confirmation of gene expression changes. *A* and *B,* TaqMan QRT-PCR was performed on cDNAs generated from 21 nulliparous and 21 parous Lewis rat mammary samples. Each reaction was performed in duplicate. Expression values for each gene were normalized to *B2m. A,* relative expression of parity up-regulated genes. *White columns,* mean expression in nulliparous samples normalized to 1.0 for each gene; *gray columns,* mean expression of each gene in parous relative to nulliparous samples; *bars,* ±SE. *B,* relative expression of parity down-regulated genes. *White columns,* mean expression of each gene in nulliparous relative to parous samples; *gray columns,* mean expression in parous samples normalized to 1.0 for each gene; *bars,* ±SE. *P* values were generated using a one-tailed, unpaired Student's *t* test. *C,* Mason's trichrome staining. Abdominal mammary glands from nulliparous and parous Lewis rats were stained with Mason's trichrome to assess total collagen present in the ECM surrounding epithelial structures. Images are representative of distal structures in the mammary glands of three nulliparous and three parous Lewis rats (original magnification, ×200).

plausible mechanism by which parity may confer protection against breast cancer.

The functional unit of the mammary gland consists of a complex stroma that surrounds the epithelial compartment. Stromal-epithelial interactions play a prominent role, not only in mammary development, but also in tumorigenesis (28). Fibroblasts represent the most prominent cell type of the periductal stroma and, in addition to secreting growth factors that activate epithelial receptors, they are the primary synthesizers of ECM constituents such as fibronectin, collagen, and proteoglycans. Accumulating evidence indicates that stromal constituents, including fibroblasts and ECM structural components, could have differential effects on epithelial cells depending on the

source of the tissue from which they are isolated (41). Consistent with this, Schedin et al. have shown that the ability of mammary epithelial cells to form ductal structures in culture is markedly influenced by the developmental context of the ECM in which they are cultured (29). Further support for the role of ECM regulation in parity-induced protection against breast cancer comes from our observation that parous mammary glands exhibit decreased trichrome staining as well as persistent down-regulation of ECM structural and regulatory genes. Because cross-talk between epithelial and stroma cells occurs through local growth factors and their receptors (42), it is possible that parity-induced down-regulation of *Areg* and *Igf-I* in combination with up-regulation of *Tgfb3* may alter stromal-epithelial interactions in such a way as to decrease susceptibility to mammary carcinogenesis.

Finally, it is interesting to speculate that parity-induced changes in the ECM may be related to measures of breast cancer risk associated with mammographic breast density. Increased mammographic density has been consistently shown to correlate with high breast cancer risk (43). Mammographic density has also been reported to be negatively correlated with parity (44). Although breast density was initially believed to reflect the epithelial content of the breast, current evidence suggests that ECM composition—in particular collagen and proteoglycans such as lumican—may be the primary determinant of mammographic density (44, 45). Intriguingly, recent studies have implicated the ratio of serum IGF-I to IGFBP3 as a major determinant of mammographic density (46). Consistent with this, Guo et al. found increased IGF-I tissue staining in samples from women with increased breast density (45). Our findings support the hypothesis that parity decreases Igf-I expression and activity and diminishes the expression of selected ECM structural components. Together, these changes may lead to decreases in both mammographic breast density and breast cancer risk. Validation of this hypothesis will require confirmation that parity alters local IGF-I levels and mammographic breast density in women, and that modulation of Igf-I in rodent models will alter breast density as well as pregnancy-induced protection against breast cancer.

In summary, the results presented in this study extend previous observations that parity results in local changes in growth factor gene expression in the mammary gland. We hypothesize that the evolutionarily conserved parity-induced alterations in gene expression identified in this study result in the modification of the extracellular environment and changes in stromal-epithelial interactions. We hypothesize that the ultimate effect of these changes is to create a tumor suppressive state, thereby providing a potential mechanism to explain parity-induced protection against mammary tumorigenesis. Whether analogous parity-induced changes occur in the human breast remains an important yet unresolved question.

References

1. Chodosh LA, D'Cruz CM, Gardner HP, et al. Mammary gland development, reproductive history, and breast cancer risk. Cancer Res 1999;59:1765–71.
2. MacMahon B, Cole P, Lin TM, et al. Age at first birth and breast cancer risk. Bull World Health Organ 1970;43: 209–21.
3. Layde PM, Webster LA, Baughman AL, Wingo PA, Rubin GL, Ory HW. The independent associations of parity, age at first full term pregnancy, and duration of breastfeeding with the risk of breast cancer. Cancer and Steroid Hormone Study Group. J Clin Epidemiol 1989;42: 963–73.
4. Russo J, Moral R, Balogh GA, Mailo D, Russo IH. The protective role of pregnancy in breast cancer. Breast Cancer Res 2005;7:131–42.
5. Sivaraman L, Medina D. Hormone-induced protection against breast cancer. J Mammary Gland Biol Neoplasia 2002;7:77–92.
6. D'Cruz CM, Moody SE, Master SR, et al. Persistent parity-induced changes in growth factors, TGF-β3, and differentiation in the rodent mammary gland. Mol Endocrinol 2002;16:2034–51.
7. Thordarson G, Jin E, Guzman RC, Swanson SM, Nandi S, Talamantes F. Refractoriness to mammary tumorigenesis in parous rats: is it caused by persistent changes in the hormonal environment or permanent biochemical alterations in the mammary epithelia? Carcinogenesis 1995;16:2847–53.
8. Russo J, Gusterson BA, Rogers AE, Russo IH, Wellings SR, van Zwieten MJ. Comparative study of human and rat mammary tumorigenesis. Lab Invest 1990;62:244–78.
9. Sivaraman L, Stephens LC, Markaverich BM, et al. Hormone-induced refractoriness to mammary carcinogenesis in Wistar-Furth rats. Carcinogenesis 1998;19: 1573–81.
10. Yang J, Yoshizawa K, Nandi S, Tsubura A. Protective effects of pregnancy and lactation against N-methyl-N-nitrosourea-induced mammary carcinomas in female Lewis rats. Carcinogenesis 1999;20:623–8.
11. Rajkumar L, Guzman RC, Yang J, Thordarson G, Talamantes F, Nandi S. Short-term exposure to pregnancy levels of estrogen prevents mammary carcinogenesis. Proc Natl Acad Sci U S A 2001;98:11755–9.
12. Guzman RC, Yang J, Rajkumar L, Thordarson G, Chen X, Nandi S. Hormonal prevention of breast cancer: mimicking the protective effect of pregnancy. Proc Natl Acad Sci U S A 1999;96:2520–5.
13. Medina D, Smith GH. Chemical carcinogen-induced tumorigenesis in parous, involuted mouse mammary glands. J Natl Cancer Inst 1999;91:967–69.
14. Medina D, Kittrell FS. p53 function is required for hormone-mediated protection of mouse mammary tumorigenesis. Cancer Res 2003;63:6140–3.
15. Ginger MR, Gonzalez-Rimbau MF, Gay JP, Rosen JM. Persistent changes in gene expression induced by estrogen and progesterone in the rat mammary gland. Mol Endocrinol 2001;15:1993–2009.

16. Colditz GA, Rosner BA, Chen WY, Holmes MD, Hankinson SE. Risk factors for breast cancer according to estrogen and progesterone receptor status. J Natl Cancer Inst 2004;96:218–28.
17. Turcot-Lemay L, Kelly PA. Response to ovariectomy of N-methyl-N-nitrosourea-induced mammary tumors in the rat. J Natl Cancer Inst 1981;66:97–102.
18. Master SR, Stoddard AJ, Bailey LC, Pan TC, Dugan KD, Chodosh LA. Genomic analysis of early murine mammary gland development using novel probe-level algorithms. Genome Biol 2005;6:R20.
19. Gentleman RC, Carey VJ, Bates DM, et al. Bioconductor: open software development for computational biology and bioinformatics. Genome Biol 2004;5:R80.
20. Phang TL, Neville MC, Rudolph M, Hunter L. Trajectory clustering: a non-parametric method for grouping gene expression time courses, with applications to mammary development. Pac Symp Biocomput 2003;351–62.
21. Waha A, Sturne C, Kessler A, et al. Expression of the ATM gene is significantly reduced in sporadic breast carcinomas. Int J Cancer 1998;78:306–9.
22. Ito K, Fujimori M, Nakata S, et al. Clinical significance of the increased multidrug resistance-associated protein (MRP) gene expression in patients with primary breast cancer. Oncol Res 1998;10:99–109.
23. Gould MN, Zhang R. Genetic regulation of mammary carcinogenesis in the rat by susceptibility and suppressor genes. Environ Health Perspect 1991;93:161–7.
24. Flo TH, Smith KD, Sato S, et al. Lipocalin 2 mediates an innate immune response to bacterial infection by sequestering iron. Nature 2004;432:917–21.
25. Elliott MB, Tebbey PW, Pryharski KS, Scheuer CA, Laughlin TS, Hancock GE. Inhibition of respiratory syncytial virus infection with the CC chemokine RANTES (CCL5). J Med Virol 2004;73:300–8.
26. Branger J, Florquin S, Knapp S, et al. LPS-binding protein-deficient mice have an impaired defense against Gram-negative but not Gram-positive pneumonia. Int Immunol 2004;16:1605–11.
27. Flint DJ, Beattie J, Allan GJ. Modulation of the actions of IGFs by IGFBP-5 in the mammary gland. Horm Metab Res 2003;35:809–15.
28. Tlsty TD, Hein PW. Know thy neighbor: stromal cells can contribute oncogenic signals. Curr Opin Genet Dev 2001;11:54–9.
29. Schedin P, Mitrenga T, McDaniel S, Kaeck M. Mammary ECM composition and function are altered by reproductive state. Mol Carcinog 2004;41:207–20.
30. Cheng N, Bhowmick NA, Chytil A, et al. Loss of TGF-β type II receptor in fibroblasts promotes mammary carcinoma growth and invasion through upregulation of TGF-α-, MSP- and HGF-mediated signaling networks. Oncogene 2005;24:5053–68.
31. Pierce DF, Jr., Gorska AE, Chytil A, et al. Mammary tumor suppression by transforming growth factor β1 transgene expression. Proc Natl Acad Sci U S A 1995;92: 4254–8.
32. Ma L, de Roquancourt A, Bertheau P, et al. Expression of amphiregulin and epidermal growth factor receptor

in human breast cancer: analysis of autocrine and stromal-epithelial interactions. J Pathol 2001;194:413–9.
33. Menashi S, Serova M, Ma L, Vignot S, Mourah S, Calvo F. Regulation of extracellular matrix metalloproteinase inducer and matrix metalloproteinase expression by amphiregulin in transformed human breast epithelial cells. Cancer Res 2003;63:7575–80.
34. Schernhammer ES, Holly JM, Pollak MN, Hankinson SE. Circulating levels of insulin-like growth factors, their binding proteins, and breast cancer risk. Cancer Epidemiol Biomarkers Prev 2005;14:699–704.
35. Laban C, Bustin SA, Jenkins PJ. The GH-IGF-I axis and breast cancer. Trends Endocrinol Metab 2003;14:28–34.
36. Thordarson G, Slusher N, Leong H, et al. Insulin-like growth factor (IGF)-I obliterates the pregnancy-associated protection against mammary carcinogenesis in rats: evidence that IGF-I enhances cancer progression through estrogen receptor-α activation via the mitogen-activated protein kinase pathway. Breast Cancer Res 2004;6:R423–36.
37. Thordarson G, Semaan S, Low C, et al. Mammary tumorigenesis in growth hormone deficient spontaneous dwarf rats; effects of hormonal treatments. Breast Cancer Res Treat 2004;87:277–90.
38. Hadsell DL, Bonnette SG. IGF and insulin action in the mammary gland: lessons from transgenic and knockout models. J Mammary Gland Biol Neoplasia 2000;5:19–30.
39. Gallego MI, Binart N, Robinson GW, et al. Prolactin, growth hormone, and epidermal growth factor activate Stat5 in different compartments of mammary tissue and exert different and overlapping developmental effects. Dev Biol 2001;229:163–75.
40. Marshman E, Green KA, Flint DJ, White A, Streuli CH, Westwood M. Insulin-like growth factor binding protein 5 and apoptosis in mammary epithelial cells. J Cell Sci 2003;116:675–82.
41. Barcellos-Hoff MH, Ravani SA. Irradiated mammary gland stroma promotes the expression of tumorigenic potential by unirradiated epithelial cells. Cancer Res 2000;60:1254–60.
42. Bhowmick NA, Neilson EG, Moses HL. Stromal fibroblasts in cancer initiation and progression. Nature 2004;432:332–7.
43. Tice JA, Cummings SR, Ziv E, Kerlikowske K. Mammographic breast density and the Gail model for breast cancer risk prediction in a screening population. Breast Cancer Res Treat 2005;94:115–22.
44. Li T, Sun L, Miller N, et al. The association of measured breast tissue characteristics with mammographic density and other risk factors for breast cancer. Cancer Epidemiol Biomarkers Prev 2005;14:343–9.
45. Guo YP, Martin LJ, Hanna W, et al. Growth factors and stromal matrix proteins associated with mammographic densities. Cancer Epidemiol Biomarkers Prev 2001;10:243–8.
46. Diorio C, Pollak M, Byrne C, et al. Insulin-like growth factor-I, IGF-binding protein-3, and mammographic breast density. Cancer Epidemiol Biomarkers Prev 2005;14:1065–73.

Correction

Correction: Pregnancy-Induced Protection against Mammary Tumorigenesis

In the article on pregnancy-induced protection against mammary tumorigenesis in the June 15, 2006 issue of *Cancer Research* (1), the parity status of six of the 43 arrays used to derive the 70-gene expression signature was misclassified through an error in data entry. These arrays represented six of the 14 arrays run for Fischer 344 rats. The remaining 37 arrays for the Lewis, Wistar-Furth, Copenhagen, and Fischer 344 mammary samples were properly classified, as were the independent Lewis rat and FVB mouse samples used to validate the findings. This misclassification both obscured genuine parity-induced changes in the Fischer 344 strain and added biological noise due to genes that were covarying but unrelated to parity. As a consequence, after correcting the parity status for the six Fischer 344 arrays and applying the same analytical criteria described in the article, the authors found that the core parity-induced gene expression signature was reduced from 70 to 47 genes. Similar to the original 70-gene signature, this 47-gene signature is sufficient to distinguish between independent nulliparous and parous samples from all rat and mouse strains

analyzed in the article. Corrected versions of Tables 1 and 2 appear below.

Each of the five originally identified functional gene categories (Tgf-β3, differentiation, immune markers, growth hormone/Igf-1 axis, and extracellular matrix components) are retained within this signature. Genes lost from the original 70-gene signature remain significantly altered in two of the four rat strains and are still plausible candidates for contributing to parity-induced protection against mammary tumorigenesis. Notably, a role for downregulation of *Ghr*, which is not included in the corrected signature, in parity-induced protection is still supported by the FVB mouse data and the QRT-PCR analysis of independent Lewis rat samples presented in the article. Also consistent with a role for the GH/Igf-1 pathway in parity-induced protection, *Igf-1* remains downregulated — and *Igfbp5* remains upregulated — on the corrected list of genes.

Overall, despite the reassignment of six samples, the conclusions of the article remain unaltered. Moreover, as a primary goal of the original article was to narrow down the list of genes to those most robustly associated with parity-induced protection, the corrected signature accomplishes this and provides an even

Table 1. Genes up-regulated in parous rats

Gene name	Symbol	Gene ID	Function	Category	Fold-change G1P1 versus G0P0				
					Lewis	WF	F344	Cop	Median
Immunoglobulin heavy chain	*Igha*	314487	Immunoglobulin	Immune	39.4	25.4	12.4	6.9	18.9
Casein beta	*Csn2*	29173	Milk protein	Differentiation	8.0	5.2	1.6	1.5	3.4
IgM light chain		287965	Immunoglobulin	Immune	2.5	3.8	2.0	1.6	2.2
Insulin-like growth factor binding protein 5	*Igfbp5*	25285	Igf1-binding	Growth factor/ECM	2.4	1.4	1.1	2.7	1.9
Casein gamma	*Csng*	114595	Milk protein	Differentiation	3.1	1.9	1.8	0.9	1.9
Lipopolysaccharide binding protein	*Lbp*	29469	Antibacterial	Immune	2.1	1.3	1.0	2.0	1.7
Matrix metalloproteinase 12	*Mmp12*	117033	Proteolysis	ECM/Immune	2.6	1.4	1.6	1.3	1.5
Carbonic anhydrase 2	*Ca2*	54231	Carbon metabolism	Metabolism	1.5	1.5	1.5	1.1	1.5
Fatty acid synthase	*Fasn*	50671	Fatty acid biosynthesis	Metabolism/Differentiation	2.0	1.6	1.3	0.9	1.5
Cytochrome P450, family 4, subfamily b,1	*Cyp4b1*	24307	Monooxygenase activity	Metabolism	1.6	1.5	1.4	1.2	1.4
Transforming growth factor, beta 3	*Tgfb3*	25717	Cell growth/proliferation	Tgf-β	1.5	1.3	0.9	1.4	1.4
Thioesterase domain containing 1	*Thedc1*	64669	Fatty acid biosynthesis	Metabolism/Differentiation	1.9	1.2	0.8	1.5	1.3
Malic enzyme 1	*Me1*	24552	Pyruvate synthesis	Metabolism	1.3	1.4	1.4	1.1	1.3
Phosphodiesterase 4B	*Pde4b*	24626	cAMP phoshodiesterase	Signal transduction	1.3	1.4	0.8	1.4	1.3
Polymeric immunoglobulin receptor	*Pigr*	25046	Trancytosis	Immune	1.7	1.4	1.2	1.1	1.3
Kruppel-like factor 9	*Klf9*	117560	Transcription Factor	Signal transduction	1.3	1.4	1.2	1.1	1.3
Matrix metalloproteinase 11	*Mmp11*	25481	Proteolysis	ECM	1.2	1.2	1.2	1.2	1.2

NOTE: Genes identified as up-regulated by at least 1.2-fold in three out of four rat strains as a result of parity are reported from highest to lowest median fold-change. Gene names and symbols are reported based on the Rat Genome Database, and Gene ID according to Entrez Gene. Gene functions and categories are based upon GeneOntology.

Abbreviations: WF, Wistar-Furth; F344, Fischer 344; Cop, Copenhagen.

smaller overlap of evolutionarily conserved gene expression changes associated with parity-induced protection against mammary tumorigenesis.

1. Blakely CM, Stoddard AJ, Belka GK, Dugan KD, Notarfrancesco KL, Moody SE, D'Cruz CM, Chodosh LA. Hormone-induced protection against mammary tumorigenesis is conserved in multiple rat strains and identifies a core gene expression signature induced by pregnancy. Cancer Res 2006;66:6421–31.

Table 2. Genes down-regulated in parous rats

Gene name	Symbol	Gene ID	Function	Category	Fold-change G0P0 versus G1P1				
					Lewis	WF	F344	Cop	Median
Periostin	*Postn*	361945	Cell adhesion	ECM	1.9	2.1	1.6	2.2	2.0
Amphiregulin	*Areg*	29183	Epidermal growth factor receptor ligand	Growth factor	3.5	2.1	1.9	1.9	2.0
Cellular retinoic acid binding protein I	*Crabp1*	25061	Retinoic acid receptor signaling	Signal transduction	1.8	2.1	1.3	1.5	1.7
Glycosylation dependent cell adhesion molecule 1	*Glycam1*	25258	Selectin ligand	Differentiation	0.5	2.2	1.3	1.7	1.5
Secreted acidic cysteine rich glycoprotein	*Sparc*	24791	ECM Formation	ECM	1.9	1.3	1.1	1.7	1.5
Lumican	*Lum*	81682	Proteoglycan	ECM	1.3	1.5	1.5	1.4	1.5
3-hydroxy-3-methylglutaryl-Coenzyme A synthase 2	*Hmgcs2*	24450	Cholesterol/ketone body biosynthesis	Metabolism	2.9	1.3	1.6	1.0	1.5
Fibronectin 1	*Fn1*	25661	Integrin signaling	ECM	1.4	1.3	1.3	1.6	1.4
Cbp/p300-interacting transactivator with Glu/Asp-rich carboxy-terminal domain	*Cited1*	64466	Transcription factor	Signal transduction	1.4	1.9	1.3	1.3	1.4
Ectonucleotide pyrophosphatase/phosphodiesterase 2	*Enpp2*	84050	Lysophospholipase	Cell motility	1.7	1.4	0.8	1.3	1.4
Insulin-like growth factor 1	*Igf1*	24482	Cell proliferation/survival	Growth factor	1.7	1.2	1.1	1.5	1.3
Sushi-repeat-containing protein	*Sprx*	64316			1.3	1.3	1.1	1.5	1.3
Lectin, galactose binding, soluble 1	*Lgals1*	56646	Integrin signaling	ECM	1.5	1.2	0.8	1.4	1.3
A kinase (PRKA) anchor protein (gravin) 12	*Akap12*	83425	Scaffolding protein	Signal transduction	1.2	1.6	1.2	1.3	1.3
Lectin, galactose binding, soluble 7	*Lgals7*	29518	Galactose binding		1.1	1.8	1.4	1.2	1.3
Tropomyosin 1, alpha	*Tpm1*	24851	Actin binding		1.1	1.3	1.3	1.3	1.3
Activity and neurotransmitter induced early gene protein 4	*Ania4*	360341	CAM kinase	Kinase	1.5	1.2	1.0	1.3	1.3
Cytosolic cysteine dioxygenase 1	*Cdo1*	81718	Cysteine metabolism	Metabolism	1.5	1.2	0.8	1.3	1.3
Carbonic anhydrase 3	*Ca3*	54232	Carbon metabolism	Metabolism	1.8	1.2	0.8	1.3	1.2
CD74 antigen	*Cd74*	25599		Immune	1.2	1.2	1.3	1.3	1.2
Tubulin, alpha 1	*Tuba1*	64158	Microtubule component	Cell structure	1.5	1.2	0.9	1.2	1.2
Similar to RIKEN cDNA 6330406I15	*RGD1307396*	360757			1.6	1.2	1.0	1.3	1.2
Collagen, type 1, alpha 1	*Col1a1*	29393	ECM structural protein	ECM	0.9	1.2	1.2	1.6	1.2
Phosphoglycerate kinase 1	*Pgk1*	24644	Phosphoprotein glycolysis	Metabolism	1.6	1.2	0.9	1.2	1.2
Annexin A5	*Anxa5*	25673	Calcium ion binding		1.6	1.2	0.8	1.2	1.2
Prohibitin	*Phb*	25344	Regulation of cell cycle	Signal transduction	1.3	1.2	1.2	1.1	1.2
Valosin-containing protein	*Vcp*	116643	Endoplasmic reticulum protein catabolism		1.2	1.2	1.2	1.2	1.2
Tropomyosin 4	*Tpm4*	24852	Actin binding		1.1	1.3	1.2	1.2	1.2
Tubulin, beta 5	*Tubb5*	29214	Microtubule component	Cell structure	1.1	1.3	1.2	1.2	1.2
MORF-related gene X	*Morf412*	317413			1.4	1.2	1.0	1.2	1.2

NOTE: Genes identified as down-regulated by at least 1.2-fold in three out of four rat strains as a result of parity are reported from highest to lowest median fold-change. Gene names and symbols are reported based on the Rat Genome Database, and Gene ID according to Entrez Gene. Gene functions and categories are based upon GeneOntology.

Abbreviations: WF, Wistar-Furth; F344, Fischer 344; Cop, Copenhagen.

Research article

Dense breast stromal tissue shows greatly increased concentration of breast epithelium but no increase in its proliferative activity

Debra Hawes[1], Susan Downey[2], Celeste Leigh Pearce[3], Sue Bartow[4], Peggy Wan[3], Malcolm C Pike[3] and Anna H Wu[3]

[1]Department of Pathology, Keck School of Medicine, University of Southern California, 2011 Zonal Avenue, Los Angeles, CA 90089, USA
[2]Department of Surgery, Keck School of Medicine, University of Southern California, 1510 San Pablo Street, Los Angeles, CA 90033, USA
[3]Department of Preventive Medicine, Keck School of Medicine, University of Southern California/Norris Comprehensive Cancer Center, 1441 Eastlake Avenue, Los Angeles, CA 90033, USA
[4]107 Stark Mesa, Carbondale, CO 81623, USA

Corresponding author: Malcolm C Pike, mcpike@usc.edu

Abstract

Introduction Increased mammographic density is a strong risk factor for breast cancer. The reasons for this are not clear; two obvious possibilities are increased epithelial cell proliferation in mammographically dense areas and increased breast epithelium in women with mammographically dense breasts. We addressed this question by studying the number of epithelial cells in terminal duct lobular units (TDLUs) and in ducts, and their proliferation rates, as they related to local breast densities defined histologically within individual women.

Method We studied deep breast tissue away from subcutaneous fat obtained from 12 healthy women undergoing reduction mammoplasty. A slide from each specimen was stained with the cell-proliferation marker MIB1. Each slide was divided into (sets of) areas of low, medium and high density of connective tissue (CT; highly correlated with mammographic densities). Within each of the areas, the numbers of epithelial cells in TDLUs and ducts, and the numbers MIB1 positive, were counted.

Results The relative concentration (RC) of epithelial cells in high compared with low CT density areas was 12.3 (95% confidence interval (CI) 10.9 to 13.8) in TDLUs and 34.1 (95% CI 26.9 to 43.2) in ducts. There was a much smaller difference between medium and low CT density areas: RC = 1.4 (95% CI 1.2 to 1.6) in TDLUs and 1.9 (95% CI 1.5 to 2.3) in ducts. The relative mitotic rate (RMR; MIB1 positive) of epithelial cells in high compared with low CT density areas was 0.59 (95% CI 0.53 to 0.66) in TDLUs and 0.65 (95% CI 0.53 to 0.79) in ducts; the figures for the comparison of medium with low CT density areas were 0.58 (95% CI 0.48 to 0.70) in TDLUs and 0.66 (95% CI 0.44 to 0.97) in ducts.

Conclusion Breast epithelial cells are overwhelmingly concentrated in high CT density areas. Their proliferation rate in areas of high and medium CT density is lower than that in low CT density areas. The increased breast cancer risk associated with increased mammographic densities may simply be a reflection of increased epithelial cell numbers. Why epithelium is concentrated in high CT density areas remains to be explained.

Introduction

On a mammogram, fat appears radiolucent or dark, whereas stromal and epithelial tissue appears radio-dense or white. The amount of mammographic density is a strong independent predictor of breast cancer risk [1,2]. The biological basis for this increased risk is poorly understood. A critical question is whether densities are directly related to risk or are simply a marker of risk. We addressed this question recently by studying the location of small ductal carcinoma *in situ* (DCIS) lesions as revealed by microcalcifications, and showed that such DCIS occurs overwhelmingly in the mammographically dense areas of the breast [3]. Most DCIS lesions in our study

---

a_H, a_L, a_M = the areas of the slide classified as being of high, low and medium CT density (in μm^2); CI = confidence interval; CT = connective tissue; DAB = 3,3'-diaminobenzidine tetrahydrochloride; DCIS = ductal carcinoma *in situ*; n_H, n_L, n_M = the numbers of epithelial cells staining positive for MIB1 within high, low and medium CT density areas; RC = relative concentration; RMR = relative mitotic rate; TDLU = terminal duct lobular unit; t_H, t_L, t_M = the numbers of epithelial cells within high, low and medium CT density areas;

Table 1

Relation between relative concentration of epithelial cells and connective tissue density

CT density	RC	95% CI	p
TDLUs			
Low	1.0		
Medium	1.4	1.2–1.6	<0.001
High	12.3	10.9–13.8	<0.001
Ducts			
Low	1.0		
Medium	1.9	1.5–2.3	<0.001
High	34.1	26.9–43.2	<0.001

CI, confidence interval; CT, connective tissue; RC, relative concentration (per unit area); TDLUs, terminal duct lobular units.

occurred in the lateral-superior quadrant, as has been found in previous studies [4], and 'correlated strongly with the average percentage density in the different mammographic quadrants' [3]. Pre-DCIS mammograms that were taken on average about two years previously showed that the areas subsequently exhibiting DCIS were clearly dense at the time of the earlier mammogram, and this suggests that this relationship was not brought about by the presence of the DCIS. The reasons for these findings are not clear; two obvious possibilities are increased epithelial cell proliferation in mammographically dense areas of the breast and increased breast epithelium in women with mammographically dense breasts. Two groups have investigated the relationship between the amount of mammographic density of a woman and the amount of her breast epithelial tissue [5,6]. Alowami and colleagues [5] used tissue obtained from biopsies investigating breast lesions that were subsequently diagnosed as benign or pre-invasive breast disease; they studied tissue 'distant from the diagnostic lesion' without reference to its location as regards mammographic density (that is, 'random' tissue). They found that the median density of duct lobular units was 28% higher in breasts whose overall mammographic density was 50% or more ($n = 27$) than in breasts whose overall mammographic density was less than 25% ($n = 35$); this result was not statistically significant and the result was described as showing 'no difference in the density of epithelial components' [5]. Li and colleagues [6] also found in their much larger study ($n = 236$) of 'random' breast tissue collected from normal women by Bartow and colleagues [7] in their autopsy study of accidental deaths in New Mexico that women with high mammographic density had greater amounts of epithelial tissue (as measured by area of epithelial nuclear staining) and the result was highly statistically significant. Breast epithelial proliferation rates as they relate to mammographic densities in healthy women have not been well studied [8]. We have addressed these questions by studying the number of epithelial cells in terminal duct lobular units (TDLUs) and in breast ducts, and their respective prolif-

eration rates as they relate to local histological breast densities within individual women.

Materials and methods

We retrospectively identified 15 consecutive healthy women who had undergone a reduction mammoplasty performed by one of us (SD) at the University of Southern California medical facilities. The study protocol was approved by the Institutional Review Board of the University of Southern California School of Medicine.

For each participant we obtained the formalin-fixed paraffin-embedded block of tissue that had been routinely processed and saved from her surgery. A single slide was cut from each block and stained with the proliferation marker MIB1 (Bio-Genex Laboratories, San Ramon, CA, USA). The slides were prepared in accordance with our previously published protocol [9]; the chromogen used was 3,3'-diaminobenzidine tetrahydrochloride (DAB). On microscopic examination one of the slides contained skin and two other slides showed areas of disintegration; all three were deemed unsuitable for study.

Each of the remaining 12 slides was divided into (sets of) areas of low, medium and high density of connective tissue (CT) (highly correlated with densities as defined by mammographic criteria [10]); see Figure 1. The total size of each of the three areas (in μm^2), and within each of the three areas the numbers of epithelial cells in TDLUs and ducts and the numbers that were MIB1 positive, were counted with the help of an automated microscope system that digitized the images and permitted the outlining of relevant areas on a high-resolution computer screen (ACIS II; Clarient, Inc., San Juan Capistrano, CA, USA). The total numbers of epithelial cells in different outlined areas within the CT density-defined areas was then automatically counted by the ACIS II nuclear counting software program, which is based on color identification. Hematoxylin was used to counterstain the MIB1-negative nuclei blue, and the DAB chromogen marked the MIB1-positive nuclei brown.

Figure 1
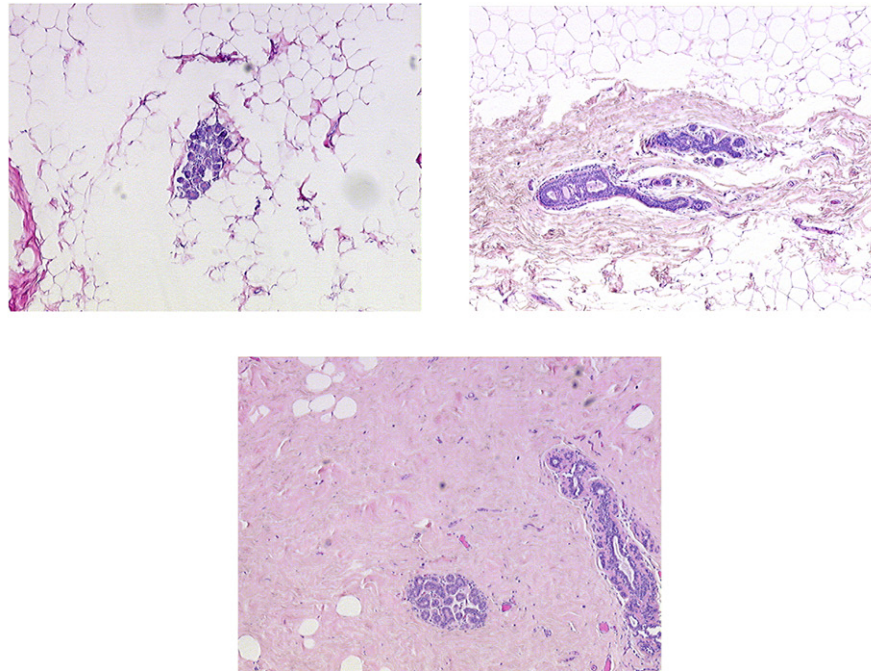
Example of areas of low, medium (upper right) and high (lower center) CT density.

The software calculated the numbers of MIB1-negative and MIB1-positive cells on the basis of these color differences.

Statistical analysis

For each slide, and separately for TDLU and ductal cells, three sets of values were obtained: first, the areas of the slide classified as being of low, medium or high CT density (a_L, a_M and a_H in μm^2); second, the numbers of epithelial cells within these areas (t_L, t_M and t_H); and third, the numbers of these epithelial cells staining positive for MIB1 (n_L, n_M and n_H). On the null hypothesis of no association between the t's and the a's – that is, no association between the numbers of epithelial cells and the CT density of the local tissue – the expected value of the t's is simply proportional to the related a's, so that, for example, the expected value of t_H is $(t_L + t_M + t_H) \times a_H/(a_L + a_M + a_H)$. Similarly, on the null hypothesis of no association between MIB1 positivity as a proportion of epithelial cells and the CT density of the local tissue, the expected value of the n's is simply proportional to the related t's, so that, for example, the expected value of n_H is $(n_L + n_M + n_H) \times t_H/(t_L + t_M + t_H)$. We analyzed these data with standard statistical software as implemented in the STATA statistical software package (procedure cs; Stata Corporation, Austin, TX, USA); the ratios of epithelial concentration (cells per unit area) and the ratios of proportions of epithelial cells staining positive for MIB1 are the measures of effect. All statistical significance levels (p values) quoted are two-sided.

Results

The 12 subjects included in the analysis were aged 18 to 60 years with a median age of 33 years; only one subject was aged 50 years or older.

Areas of the slides of low CT density comprised on average 44% of the total of areas of low plus medium plus high CT density ($a_L/(a_L + a_M + a_H)$), whereas areas of high CT density comprised on average 35% of the total area ($a_H/(a_L + a_M + a_H)$).

Table 1 shows the summary relative concentrations (RCs; ratios of cells per unit area) of epithelial cells in the three areas defined by CT density separately for TDLU cells and for ductal cells. The concentration of TDLU epithelial cells is slightly greater in the areas of medium CT density than in the areas of low CT density (RC = 1.4, 95% confidence interval (CI) 1.2 to 1.6; $p < 0.001$) but is much greater in the areas of high CT density (RC = 12.3, 95% CI 10.8 to 13.8; $p < 0.001$). The TDLU results for the individual slides (women) comparing areas of high CT density with areas of low CT density are shown in Figure 2. Although the results from individual subjects do differ somewhat, the RCs were not correlated with age (the only variable available on these women) and the summary RC seems to be a fair representation of the overall results. The results for ducts were similar.

Table 2 shows the summary relative mitotic rates (RMRs) of epithelial cells staining MIB1 positive in the three areas defined by CT density separately for TDLU cells and for ductal

Table 2

Relation between relative mitotic rate (MIB1 positive) of epithelial cells and connective tissue density

CT density	RMR	95% CI	*p*
TDLUs			
Low	1.00		
Medium	0.58	0.48–0.70	<0.001
High	0.59	0.53–0.66	<0.001
Ducts			
Low	1.00		
Medium	0.66	0.44–0.97	0.035
High	0.65	0.53–0.79	<0.001

CI, confidence interval; CT, connective tissue; RMR, relative mitotic rate; TDLUs, terminal duct lobular units.

Figure 2

RCs (with 95% CIs) of TDLU epithelial cells in high and low CT areas.

Figure 3
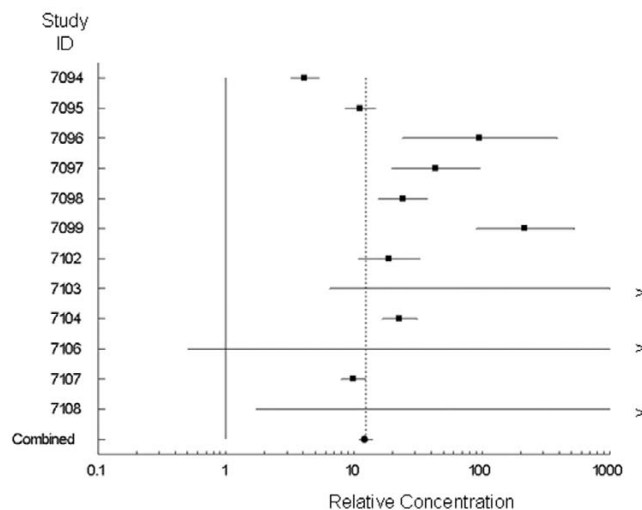
RMRs (with 95% CIs) of TDLU epithelial cells in high and low CT areas.

cells. The proportion of TDLU epithelial cells staining MIB1 positive is statistically significantly less (RMR ≈ 0.6) both in the areas of medium CT density (*p* < 0.001) and in the areas of high CT density (*p* < 0.001) than in the areas of low CT density. The median MIB1-positive proportion was about 4%. Almost all the women in this study were premenopausal on the basis of their age; this figure is close to the Ki67 figure of 4.5% given for healthy premenopausal women in the study of Hargreaves and colleagues [11]. The TDLU results for the individual slides (women) comparing areas of high CT density with areas of low CT density are shown in Figure 3. Again, although the results from individual subjects do differ somewhat, the RMRs were not correlated with age (the only variable available on these women) and the summary RMR seems to be a fair representation of the overall results. The results for ducts were again similar. There was no difference in the proliferation rates of epithelial cells in TDLUs and ducts within the same CT den-

sity area of individual women (RMR = 1.01, 95% CI 0.98 to 1.04; *p* = 0.42).
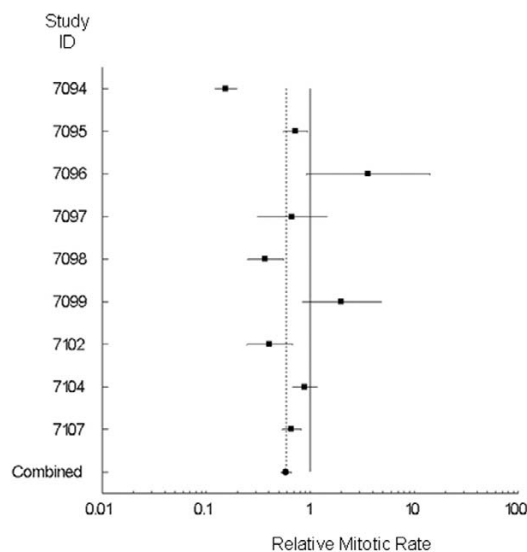
More details of the results are provided in the Additional file.

Discussion

Mammographic density is a very strong risk factor for breast cancer. The two groups of investigators [5,6] that studied random biopsies (single slides) from women with different mammographic densities found that the extent of mammographic densities was most strongly correlated with the amount of collagen on the slide. A weaker correlation was found with the amount of epithelial tissue. The findings reported here suggest that the relation between the extent of mammographic density and the amount of epithelial tissue is directly related to the increased concentration of collagen (the main component of

'connective tissue' as shown by collagen staining; see Figure 1) in women with high mammographic densities, because breast epithelium is overwhelmingly confined to areas of high CT density. In the earlier studies of random biopsies [5,6] the weaker relationship between mammographic density and epithelium concentration than between mammographic density and collagen concentration could be simply due to the much greater statistical variability of epithelial tissue in a random slide than one would see for collagen, which occupies a much greater extent of the slide. These results suggest that the increasing breast cancer risk associated with increasing mammographic density might be simply a reflection of more breast epithelial tissue.

We found that the proliferation rate of epithelial cells in areas of high CT density was much lower than in areas of low CT density, arguing against the possibility that dense stroma has a growth factor role in the increased breast cancer risk of women with mammographically dense breasts. In the study of Stomper and colleagues [8], comparison was made between single biopsies of either fat or dense areas in different women; they found no difference in the proliferation rates in the dense and fat areas. Further work is warranted but there is clearly no evidence that areas of high CT density are associated with increased proliferation.

Our results were obtained by conducting a comprehensive count of all the cells in each slide per subject (instead of counting a selected region) and allowed the comparison of proliferation rates in areas of differing CT density within an individual. This permitted us to control completely automatically for factors such as age, menopausal status, or time in the menstrual cycle in the analysis. This gave us great statistical power so that highly statistically significant results could be obtained even with small numbers of subjects.

This study used tissue obtained at reduction mammoplasty performed on women with large breasts. We do not believe that this affects the validity of our findings because the tissue samples were taken deep in the breast away from the subcutaneous fat, but this requires confirmation in future studies. Further studies are also needed relating the CT densities to such risk factors as parity and to understand the biology of the relationship between CT densities and breast epithelium.

Conclusion
The basis of the strong relationship between mammographic density and breast cancer risk may be simply that mammographically dense breasts contain more breast epithelial tissue. Why breast epithelial tissue should be associated with CT densities is not known. Does breast epithelium induce densities? Alternatively, can breast epithelium effectively survive only in areas of densities? Understanding the nature of the interaction between dense CT stroma and epithelial tissue should be a major focus of breast cancer research.

Competing interests
The authors declare that they have no competing interests.

Authors' contributions
DH, AHW, CLP and MCP participated in the design of the study. DH supervised the preparation of the slides and analyzed the slides with the ACIS II system. SD performed all the reduction mammoplasties that provided the tissues used in this analysis and consulted on the tissue obtained from reduction mammoplasties. SB consulted on the interpretation of the results and provided insight into the relationship between mammographic densities and tissue characteristics. CLP coordinated the study. MCP supervised the statistical analysis which was carried out by PW. AHW, CLP and MCP conceived of the study. MCP, DH and AHW drafted the manuscript; all authors read and approved the final manuscript.

Additional files

The following Additional files are available online:

Additional File 1
A Word file containing two tables of detailed results from this study.
See http://www.biomedcentral.com/content/supplementary/bcr1408-S1.doc

References
1. Saftlas AF, Szklo M: **Mammographic parenchymal patterns and breast cancer risk.** *Epidemiol Rev* 1987, **9:**146-174.
2. Boyd NF, Lockwood GA, Byng JW, Tritchler DL, Yaffe MJ: **Mammographic densities and breast cancer risk.** *Cancer Epidemiol Biomarkers Prev* 1998, **7:**1133-1144.
3. Ursin G, Hovanessian-Larsen L, Parisky YR, Pike MC, Wu AH: **Greatly increased occurrence of breast cancers in areas of mammographically dense tissue.** *Breast Cancer Res* 2005, **7:**R605-R608.
4. Perkins CI, Hotes J, Kohler BA, Howe HL: **Association between breast cancer laterality and tumor location, United States, 1994-1998.** *Cancer Causes Control* 2004, **15:**637-645.
5. Alowami S, Troup S, Al-Haddad S, Kirkpatrick I, Watson PH: **Mammographic density is related to stroma and stromal proteoglycan expression.** *Breast Cancer Res* 2003, **5:**R129-R135.
6. Li T, Sun L, Miller N, Nicklee T, Woo J, Hulse-Smith L, Tsao M-S, Khokha L, Martin L, Boyd N: **The association of measured breast tissue characteristics with mammographic density and other risk factors for breast cancer.** *Cancer Epidemiol Biomarkers Prev* 2005, **14:**343-349.
7. Bartow SA, Pathak DR, Black WC, Key CR, Teaf SR: **The prevalence of benign, atypical and malignant breast lesions in pop-**

ulations at different risk for breast cancer. *Cancer* 1987, **60:**2751-2760.

8. Stomper PC, Penetrante RB, Edge SB, Arredondo MA, Blumenson LE, Stewart CC: **Cellular proliferative activity of mammographic normal dense and fatty tissue determined by DNA S phase percentage.** *Breast Cancer Res Treat* 1996, **37:**229-236.

9. Shi S-R, Cote R, Chaiwun B, Young LL, Shi Y, Hawes D, Chen T, Taylor CR: **Standardization of immunochemistry based on antigen retrieval technique for routine formalin-fixed tissue sections.** *Appl Immunohistochem* 1998, **6:**89-96.

10. Bartow SA, Mettler FA, Black WC, Moskowitz M: **Correlations between radiographic patterns and morphology of the female breast.** *Prog Surg Path* 1982, **4:**263-275.

11. Hargreaves DF, Potten CS, Harding C, Shaw LE, Morton MS, Roberts SA, Howell A, Bundred NJ: **Two-week dietary soy supplementation has an estrogenic effect on normal premenopausal breast.** *J Clin Endocrinol Metab* 1999, **84:**4017-4024.

EPIDEMIOLOGY

Progesterone and estrogen receptors in pregnant and premenopausal non-pregnant normal human breast

DeShawn Taylor · Celeste Leigh Pearce · Linda Hovanessian-Larsen ·
Susan Downey · Darcy V. Spicer · Sue Bartow ·
Malcolm C. Pike · Anna H. Wu · Debra Hawes

Abstract We report here our studies of nuclear staining for the progesterone and estrogen receptors (PRA, PRB, ERα) and cell proliferation (MIB1) in the breast terminal duct lobular unit epithelium of 26 naturally cycling premenopausal women and 30 pregnant women (median 8.1 weeks gestation). Square root transformations of the PRA, PRB and ERα values, and a logarithmic transformation of the MIB1 values, were made to achieve more normal distributions of the values. PRA expression decreased from a mean of 17.8% of epithelial cells in cycling subjects to 6.2% in pregnant subjects ($P = 0.013$). MIB1 expression increased from 1.7% in cycling subjects to 16.0% in pregnant subjects ($P < 0.001$). PRB and ERα expression was slightly lower in pregnant subjects but the differences were not statistically significant. Sixteen of the non-pregnant subjects were nulliparous and ten were parous so that we had limited power to detect changes associated with parity. PRA was statistically significantly lower in parous women than in nulliparous women (32.2% in nulliparous women vs. 10.2%; $P = 0.014$). PRB (23.5 vs. 12.9%), ERα (14.4 vs. 8.6%) and MIB1 (2.2 vs. 1.2%) were also lower in parous women, but the differences were not statistically significant. The marked decreases in PRA in pregnancy and in parous women has also been found in the rat. A reduction in PRA expression may be a useful marker of the reduction in risk with pregnancy and may be of use in evaluating the effect of any chemoprevention regimen aimed at mimicking pregnancy. Short-term changes in PRA expression while the chemoprevention is being administered may be a more useful marker.

DeShawn Taylor, Celeste Leigh Pearce, Linda Hovanessian-Larsen, Susan Downey are to be considered joint first authors of this report based on their pivotal contributions to the studies reported here.

D. Taylor
Department of Obstetrics and Gynecology, Keck School of Medicine, University of Southern California, Los Angeles, CA 90033, USA

C. L. Pearce · M. C. Pike · A. H. Wu
Department of Preventive Medicine, Keck School of Medicine, University of Southern California, Los Angeles, CA 90033, USA

L. Hovanessian-Larsen
Department of Radiology, Keck School of Medicine, University of Southern California, Los Angeles, CA 90033, USA

S. Downey
Department of Surgery, Keck School of Medicine, University of Southern California, Los Angeles, CA 90033, USA

D. V. Spicer
Department of Medicine, Keck School of Medicine, University of Southern California, Los Angeles, CA 90033, USA

S. Bartow
Department of Pathology, University of New Mexico, Albuquerque, NM 87131, USA

Present Address:
S. Bartow
107 Stark Mesa, Carbondale, CO 81623, USA

D. Hawes
Department of Pathology, Keck School of Medicine, University of Southern California, Los Angeles, CA 90033, USA

M. C. Pike (✉)
USC/Norris Comprehensive Cancer Center, 1441 Eastlake Avenue, Los Angeles, CA 90033, USA
e-mail: mcpike@usc.edu

Introduction

The progesterone receptor (PR) is expressed in two isoforms, progesterone receptor A (PRA) and progesterone receptor B (PRB) [1]. Kariagina et al. [2] described the varying expression of these two receptors in the breast epithelium of nulliparous and parous rats at differing ages, and noted that the results differed radically from the results seen in mice [3]. Their major findings in rats were: (a) The percentage of lobular cells expressing PRA (PRA + cells) declined steadily from 6 weeks of age (puberty) to 14 weeks of age in nulliparous rats, was much lower during pregnancy (8–10 days of pregnancy) and only partly recovered after involution. (b) The percentage of PRB + lobular cells was relatively constant from 3 to 14 weeks of age in nulliparous rats, and was not altered during pregnancy or after involution. These authors suggested that, since human and rat mammary glands share many features [4, 5], their finding might be applicable to the human breast. These findings in rats suggested that measuring PRA may be a simple method of distinguishing a parous from a nulliparous breast, which, if substantiated in the human breast, may be most helpful as a relatively easily obtained biomarker of possible success in chemoprevention efforts aimed at achieving the protection associated with an early pregnancy.

There are few data available on PRA and PRB expression in normal human breast tissue. We report here our findings regarding PRA and PRB expression in normal human breast tissue obtained from women undergoing reduction mammoplasties as well as from women immediately after a pregnancy termination (within 10 min of the termination). We also report here our findings for estrogen receptor α (ERα) and cell proliferation in these same breast samples.

Materials and methods

Specimen collection

We retrospectively identified 13 healthy naturally cycling premenopausal women who had undergone a reduction mammoplasty and for whom we could obtain the formalin-fixed paraffin-embedded (FFPE) block of tissue saved from her surgery that had been routinely processed at the University of Southern California Department of Pathology. We also prospectively collected breast tissue (frozen within 30 min of excision) from 8 healthy premenopausal women who were undergoing reduction mammoplasty and 5 healthy volunteers and processed this tissue in a similar manner. The mammoplasty surgeries were all performed by one of us (SD) either at the University of Southern California medical facilities or at the Pacific SurgiCenter, while the tissue from the volunteers were obtained using ultrasound guided 14-gauge core needle biopsies (LHL). Women who reported current use of hormonal contraception were excluded from the current analyses.

Ultrasound guided 14-gauge core needle breast biopsy tissue was also prospectively collected from 33 women who had undergone a pregnancy termination within the preceding 10 min. Samples of these tissues were processed in a similar manner to that described above, i.e., FFPE in a routine manner at the University of Southern California Department of Pathology. Thirty samples were suitable for analysis.

An in-person interview was conducted with the prospectively recruited mammoplasty subjects, the healthy volunteers and the pregnancy termination subjects, and a telephone interview was conducted with the retrospectively recruited mammoplasty subjects. The interview collected detailed information on reproductive and menstrual factors using a structured questionnaire.

The study protocols were approved by the Institutional Review Board (IRB) of the University of Southern California Keck School of Medicine, and as appropriate, with the IRBs of St. John's Hospital and Health Center (for Pacific SurgiCenter) and of the Department of Defense Congressionally Directed Breast Cancer Research Program. The prospectively collected samples were obtained after the women had signed an informed consent agreeing to participate in this research. The women from whom the retrospectively collected samples were obtained also provided verbal informed consent agreeing to participate in this research.

Immunohistochemistry

Immunohistochemical (IHC) analysis was performed as follows: For all studies, multiple adjacent FFPE sections were cut at 5 μm, deparaffinized and hydrated. All slides were also subject to antigen retrieval which was performed by heating the slides in 10 mmol/l sodium citrate buffer (pH 6) at 110°C for 30 min in a pressure cooker in a microwave oven [6]. Endogenous peroxidase activity was blocked by incubation in 3% H_2O_2 in phosphate-buffered saline for 10 min, followed by blocking of nonspecific sites with SuperBlock blocking buffer (Pierce, Rockford, IL, USA) for 1 h both at room temperature [7].

For the single marker studies, the sections were incubated for analysis with the following antibodies: PRA, the mouse monoclonal antibody NCL-PGR-312 (Novocastra

Laboratories Ltd, Newcastle upon Tyne, UK) at a concentration of 1:5,000; PRB, the mouse monoclonal antibody NCL-PGR-B (Novocastra Laboratories Ltd, Newcastle upon Tyne, UK) at a concentration of 1:100; ERα, the mouse monoclonal antibody ER Ab-12 (Clone 6F11) (Neomarkers, Kalamazoo, MI, USA) at a concentration of 1:100; and MIB1, a proliferation marker, the mouse monoclonal antihuman Ki67 antibody (Dako Cytomation, Carpenteria, CA, USA) at a concentration of 1:500. After incubation with the primary antibodies, antibody binding was localized with the ABC staining kit from Vector Laboratories (Burlingame, CA, USA) according to the manufacturer's instructions and peroxidase activity was detected using 3,3′-diaminobenzidine substrate solution (DAB; Biocare, Concord, CA, USA). A wash step with phosphate buffer solutions (PBS) for 10 min was carried out between each step of the immunostaining. Slides were counterstained with hematoxylin and mounted in mounting medium for examination.

A selection of the slides were also double-stained to permit luminal-epithelial and myoepithelial tissue to be clearly distinguished and to evaluate the co-expression of different markers. The myoepithelial cells were detected using an antibody for smooth muscle actin (SMA; Dako Cytomation, Carpenteria, CA, USA) at a concentration of 1:4000. SMA is localized in the cytoplasm of the cells and is easily distinguished from nuclear staining; on double-stained slides actin was detected using DAB. Ferengi blue was the second chromogen for both PRA and PRB. In slides that were double-stained for PRA and PRB, PRA was stained with Ferengi Blue (Biocare, Concord, CA, USA) and PRB with DAB. No hematoxylin counterstain was applied to the double-stained slides.

In the single-marker slides, we used the Automated Cellular Imaging System II (ACIS II, Clarient, Aliso Viejo, CA, USA) to assess all terminal duct lobular units (TDLUs) on a single slide or the first 100 target areas containing TDLUs selected systematically from left to right and top to bottom on the slide if there were an excessive number of epithelial cells present. A clear distinction between luminal-epithelial cells and myoepithelial cells in TDLUs is frequently difficult to make on conventionally stained slides. For this reason we counted the total numbers of luminal-epithelial + myoepithelial cells (referred to as epithelial cells) and the percentage of them positive for the relevant marker using the ACIS II which is a cellular imaging system that digitizes the images and permits the user to identify and quantitate relevant areas on a high-resolution computer screen based on color differentiation. The ACIS II software program does not function optimally when both nuclear and cytoplasmic staining is present. Due to some cytoplasmic staining in addition to nuclear positivity found in the ERα slides from the pregnant subjects

we used conventional light microscopy and manual counting methods for assessing the TDLUs in these cases. If scant epithelial tissue was present all epithelial cells were counted, in most cases we randomly identified 300 epithelial cells, in cases with a large amount of epithelium present we counted 500 epithelial cells to avoid sampling bias. The percentage of cells positive was determined by identifying the number of cells with nuclear positivity for the selected marker versus those negative or positive.

In the double-marker slides we used the Nuance FLEX™ spectral imaging system (Cambridge Research & Instrumentation, Inc., Woburn, MA, USA) to assess the co-expression of markers on a single slide.

Statistical analysis

We analyzed these data using standard statistical software (Stata, Stata Corporation, Austin, TX, USA). Differences in expression and tests for trend in expression were tested for significance by standard t-tests and regression tests after adjustment for age and ethnicity (African American, Hispanic Whites, non-Hispanic Whites) and after transformation of the variables to achieve more normal distributions of values (square root transformations of PRA, PRB and ERα, and logarithmic transformation of MIB1). The comparison of non-pregnant to pregnant results was also adjusted for prior parity (nulliparous/parous). All statistical significance levels (P values) quoted are two sided.

Results

Non-pregnant subjects

The means (and 95% confidence intervals) of the proportion of epithelial cells with positive nuclear staining for PRA, PRB, ERα and MIB1 in non-pregnant subjects subclassified by parity (nulliparous vs. parous) are given in Table 1. The individual values are shown in Fig. 1.

Table 1 Mean (±95% CI) percentages of PRA, PRB, ERα and MIB1 nuclear staining in premenopausal non-pregnant nulliparous and parous subjects

	Nulliparous ($N = 16$)	Parous ($N = 10$)	P value
PRA	32.2 (22.6–43.4)	10.2 (3.3–20.9)	0.014
PRB	23.5 (14.6–34.5)	12.9 (4.9–24.7)	0.20
ERα	14.4 (10.4–19.0)	8.6 (4.7–13.6)	0.11
MIB1	2.2 (1.3–3.7)	1.2 (0.6–2.6)	0.26

Comparison of parous and nulliparous subjects with square root transformation of PRA, PRB and ERα values, and logarithmic transformation of MIB1 values, and adjusted for ethnicity and age
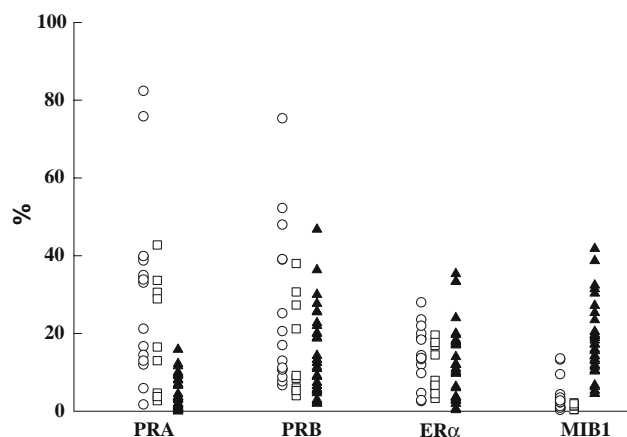
Fig. 1 Percentage of cells expressing nuclear PRA, PRB, ERα and MIB1 in premenopausal nulliparous (○), premenopausal parous (□) and pregnant (▲) women

PRA and PRB

A higher proportion of cells were positive for PRA in nulliparous compared to parous women (mean values: 32.2 vs. 10.2%; $P = 0.014$). There was also a higher proportion of cells positive for PRB in nulliparous compared to parous women (23.5 vs. 12.9%), but this difference was not statistically significant ($P = 0.20$).

PRA was expressed in the luminal epithelium but almost never expressed in the myoepithelium (Fig. 2A). PRB was expressed in both luminal epithelium and myoepithelium (Fig. 2B). The proportion of cells expressing PRB in the luminal epithelium was greater than the proportion expressing PRB in the myoepithelium, although this was difficult to assess completely satisfactorily due to the morphology of the myoepithelial cells which does not permit clear nuclear visualization in many cases.

ERα

A higher proportion of cells were positive for ERα in nulliparous compared to parous women (mean values: 14.4 vs. 8.6%), but this was also not statistically significant ($P = 0.11$). ERα was not expressed in the myoepithelium.

MIB1

A higher proportion of cells were positive for MIB1 in nulliparous women compared to parous women (mean values: 2.2 vs. 1.2%), but this was again not statistically significant ($P = 0.26$).

MIB1 expression was much lower in the myoepithelium than in the luminal epithelium.

We found no evidence that weight affected these results.
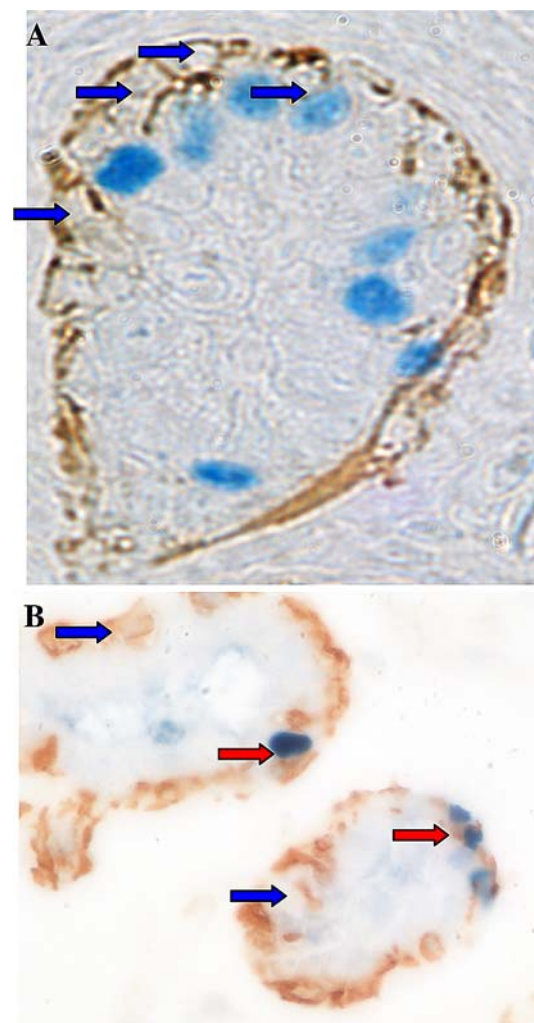
Fig. 2 **A** Double staining for PRA (*blue*) and SMA (*brown*) showing myoepithelial cells are negative for PRA (*blue arrows*). **B** Double staining for PRB (*blue*) and SMA (*brown*) showing myoepithelial cells positive (*red arrows*) and negative (*blue arrows*) for PRB

Pregnant subjects

The gestational age of the pregnant subjects varied from 5 to 23 weeks (median 8.1 weeks, interquartile range 7.2–12.0 weeks). Results are presented in Table 2.

PRA and PRB

A mean of 6.2% of epithelial cells expressed nuclear PRA. A mean of 14.2% of epithelial cells expressed nuclear PRB. As in the non-pregnant subjects, PRA was almost never expressed in the myoepithelium while PRB was expressed in both luminal epithelium and myoepithelium. In the luminal epithelium almost all cells expressing PRA expressed PRB, but many luminal epithelial cells expressed PRB without expressing PRA (Fig. 3).

Table 2 Mean (±95% CI) percentages of PRA, PRB, ERα and MIB1 nuclear staining in naturally cycling premenopausal and pregnant subjects

	Non-pregnant (N = 26)	Pregnant (N = 30)	P value
PRA	17.8 (11.5–25.6)	6.2 (3.1–10.3)	0.013
PRB	17.3 (10.9–25.2)	14.2 (9.1–20.5)	0.57
ERα	12.3 (8.1–17.5)	10.6 (7.1–14.8)	0.63
MIB1	1.7 (1.1–2.6)	16.0 (11.0–23.3)	<0.001

Comparison of pregnant and non-pregnant subjects with square root transformation of PRA, PRB, and ERα values, and logarithmic transformation of MIB1 values; and adjusted for ethnicity, age and prior parity (parous/nulliparous)
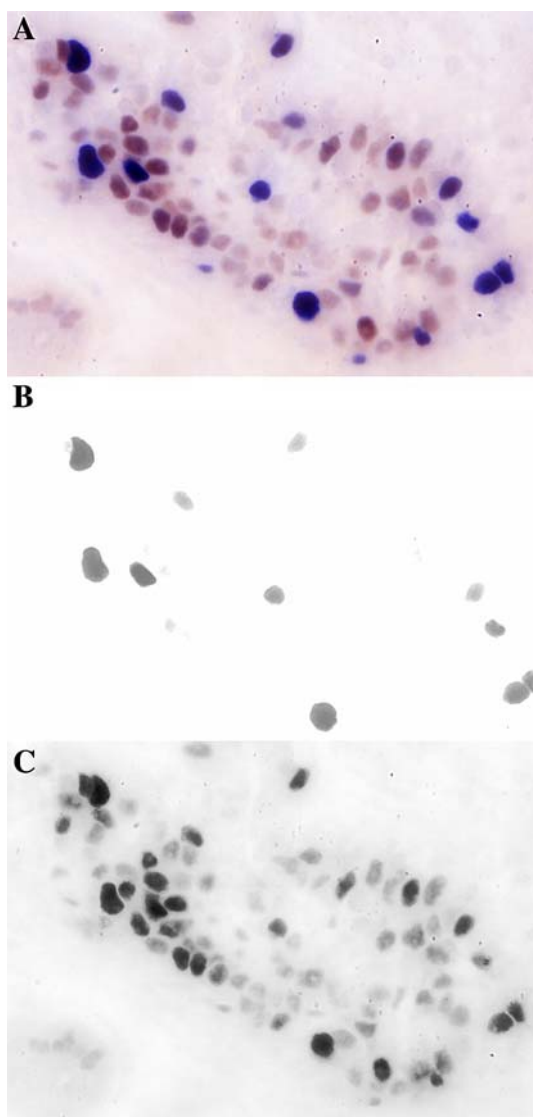
Fig. 3 A Composite spectral image showing PRA (*blue*) and PRB (*brown*) positive cells in a pregnant subject. **B** PRA positive cells only. **C** PRB positive cells only. There are many PRB positive cells that do not co-express PRA

ERα

A mean of 10.6% of epithelial cells expressed nuclear ERα. As in non-pregnant subjects, ERα was not expressed in the myoepithelium.

MIB1

A mean of 16.0% of epithelial cells expressed nuclear MIB1. As in non-pregnant subjects, MIB1 expression was much lower in the myoepithelium than in the luminal epithelium.

There was statistically significant evidence (P_{trend} = 0.043) of a decline in PRA expression with gestational age; a mean of 8.4% of cells were PRA + at a gestational age of <12 weeks vs. 1.8% at a gestational age of ≥12 weeks (Fig. 4). There was also a statistically significant (P_{trend} = 0.004) decline in ERα expression with gestational age; a mean of 13.4% at a gestational age of <12 weeks vs. 4.6% at a gestational age of ≥12 weeks (Fig. 4). PRB expression also declined with gestational age, but the effect was smaller and not statistically significant (P = 0.65). There was no effect of gestational age on MIB1 expression.

The results for PRA and MIB1 in pregnant women were markedly different from the results in non-pregnant women. PRA expression was much decreased in pregnant women [mean values: 17.8% in non-pregnant subjects vs. 6.2% in pregnant subjects (P = 0.013)], and MIB1 was much increased [1.7 vs. 16.0% (P < 0.001)].

As can be seen in Fig. 1, the results for PRA, PRB, ERα and MIB1 varied widely between different subjects. The results frequently also varied widely within a single slide; this was due in part to the positive cells tending to cluster within single TDLUs as is illustrated in Fig. 5 for ERα
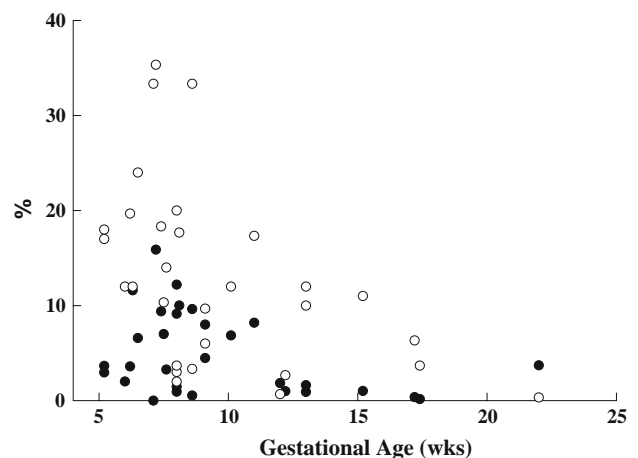
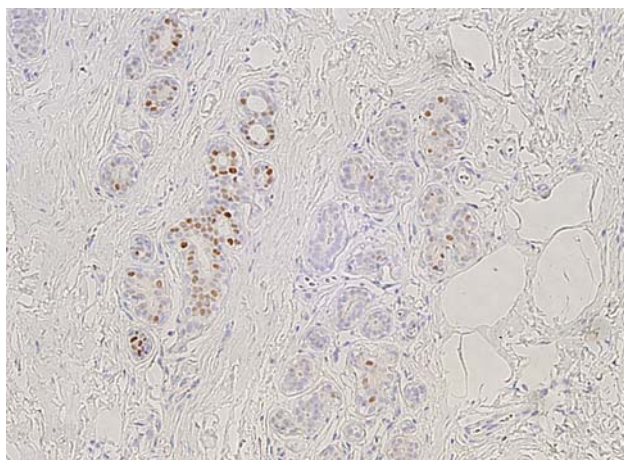**Fig. 4** Nuclear PRA (●) and ERα (○) expression in pregnant women by gestational age

Fig. 5 Number of ER positive cells (*brown nuclei*) can vary significantly between TDLUs as seen in this photomicrograph

in a non-pregnant subject and as has previously been reported [8].

PRA, PRB, ERα and MIB1 were not expressed in the non-pregnant or pregnant breast stromal fibroblasts.

Discussion

In women, a full-term birth at a young age is associated with a long-term significantly reduced risk of breast cancer and induced abortions also provide protection although to a lesser extent [9]. A clear goal for breast cancer chemoprevention efforts is to mimic the protective effect of such early pregnancies. In order to evaluate the effectiveness of any such chemoprevention effort, a biomarker indicative of achieving the desired effect must be identified.

Data from studies in rats show that expression of PRA is substantially decreased during and following pregnancy, suggesting that PRA levels may be such a marker. We have clearly shown a similar reduction in PRA expression in the human breast. PRA expression was decreased from a mean of 32.2% in nulliparous non-pregnant subjects to 6.2% in pregnant subjects, and only rose to 10.2% in parous non-pregnant subjects. PRA expression was decreased early on in pregnancy (<8 weeks gestation, see Fig. 4) and decreased further with increasing gestational age.

There was little or no change in PRB expression in pregnant subjects; this is precisely as seen in the rat [2]. PRB expression was lower in parous subjects but the difference was not statistically significant, and there was no difference in PRB expression between nulliparous and parous rats [2].

PRB was frequently expressed in myoepithelial cells as well as in luminal epithelial cells, whereas PRA expression was almost exclusively confined to luminal epithelial cells.

This effective restriction of PRA to luminal cells, while PRB was expressed in both types of epithelium, was also found in the rat [2]. In the rat, Kariagina et al. [2] found that PRB was more frequently expressed in myoepithelial cells than in luminal cells ($\sim$95 vs. $\sim$60% for all epithelial cells). We did not see this. The proportion of cells expressing PRB in the luminal epithelium appeared to be greater than the proportion expressing it in the myoepithelium.

These results differ from the results reported by Mote et al. [10] who found that PRA and PRB were co-expressed at similar levels. Their study was performed on FFPE breast tissue samples from autopsies of premenopausal women obtained some 20 years previously by one of us [11]. We were unsuccessful at staining these autopsy specimens for PRA or PRB.

Overall there was little difference in ERα expression between non-pregnant and pregnant subjects, but the results shown in Fig. 4 strongly suggest that ERα expression is increased early on in pregnancy (<8 weeks gestation) and then declines to lower levels than are seen in non-pregnant subjects. ERα expression was also lower in parous subjects but the difference was again not statistically significant. Although estrogen receptor β, ERβ, is present in a high proportion of luminal and myoepithelial cells in the normal human breast, knock-out studies have shown that ERα is the key ER in the breast [12, 13]. ERα is found in the luminal epithelium but not in any other cell type in the breast [14, 15]. Although it has been stated that all cells expressing PR also express ERα [13], this was not seen in the non-pregnant human breast in a number of studies [16–20] that found that PR was expressed more frequently than ER, although the reverse has also been reported [21, 22]. We also found that PRA was much more frequently expressed than ERα. We found some evidence of a decrease in ERα expression in parous women, but this difference was not statistically significant, and was not seen in the study of Battersby et al. [19].

MIB1 expression increased from 1.7% in non-pregnant women to 16.0% in pregnant women. The increase in breast cell proliferation in early pregnancy is, of course, well known [16, 23, 24]. MIB1 expression was also lower in parous subjects but the difference was again not statistically significant. Olsson et al. [25] also found a decrease in MIB1 expression in parous women in a small study, but this was not found in the studies reported by Longacre and Bartow [26], Anderson et al. [27] or Williams et al. [28]. Freudenhake et al. [29] reported lower MIB1 expression in parous women but their results were completely confounded with an age effect. Our finding of lower MIB1 expression in myoepithelium than in luminal epithelium confirms the results reported by Joshi et al. [30].

Epithelial staining for PRA, PRB, ERα and MIB1 were all nuclear in the non-pregnant subjects as has been

previously reported [14, 16, 23, 24]. The same held for PRA, PRB and MIB1 in pregnant subjects, but ERα showed a diffuse cytoplasmic blush in a large proportion of the pregnant subjects along with the nuclear positivity staining. Our finding of no staining of fibroblasts for PR or ERα confirms results from earlier studies [21, 31].

Experiments in mice and observations from human breast tumor studies both suggest that PRA has a deleterious effect on breast tissue [32]. In the mouse, breast development is normal in the absence of PRA, but overexpression of PRA results in a hyperplastic state [33]. Also, in PR-positive breast cancer tissue, the PRA to PRB ratio is increased with two-thirds of the tumors studied showing more PRA and a quarter showing a fourfold increase of PRA [34]. This suggests that an overabundance of PRA is a harmful characteristic and this is in line with parity being associated with a decreased risk of breast cancer and our observation of pregnancy appearing to induce long-term reductions in the expression of PRA.

A reduction in PRA expression may be a useful marker of the reduction in risk with pregnancy. However, the extent of the overlap (Fig. 1) between the results from nulliparous and parous women mean that large numbers of subjects will likely be required if it is to be used to establish such an effect with any chemoprevention regimen aimed at mimicking pregnancy. If before and after treatment samples can be obtained a change may be easier to detect. Short-term changes in PRA expression while the chemoprevention is being administered may be a more useful marker.

References

1. Vegeto E, Shahbaz MM, Wen DX, Goldman ME, O'Malley BW, McDonnell DP (1993) Human progesterone receptor A form is a cell- and promoter-specific repressor of human progesterone receptor B function. Mol Endocrinol 7:1244–1255. doi:10.1210/me.7.10.1244

2. Kariagina A, Aupperlee MD, Haslam SZ (2007) Progesterone receptor isoforms and proliferation in the rat mammary gland during development. Endocrinology 148:2723–2736. doi:10.1210/en.2006-1493

3. Aupperlee MD, Smith KT, Kariagina A, Haslam SZ (2005) Progesterone receptor isoforms A and B: temporal and spatial differences in expression during murine mammary gland development. Endocrinology 146:3577–3588. doi:10.1210/en.2005-0346

4. Russo J, Russo IH (1996) Experimentally induced mammary tumors in rats. Breast Cancer Res Treat 39:7–20. doi:10.1007/BF01806074

5. Russo IH, Russo J (1998) Role of hormones in mammary cancer initiation and progression. J Mammary Gland Biol Neoplasia 3:49–61. doi:10.1023/A:1018770218022

6. Taylor CR, Shi SR, Chen C, Young L, Yang C, Cote RJ (1996) Comparative study of antigen retrieval heating methods: microwave, microwave and pressure cooker, autoclave, and steamer. Biotech Histochem 71:263–270. doi:10.3109/10520299609117171

7. Kumar SR, Singh J, Xia G, Krasnoperov V, Hassanieh L, Ley EJ, Scehnet J, Kumar NG, Hawes D, Press MF (2006) Receptor tyrosine kinase EphB4 is a survival factor in breast cancer. Am J Pathol 169:279–293. doi:10.2353/ajpath.2006.050889

8. Shoker BS, Jarvis C, Sibson DR, Walker C, Sloane JP (1999) Oestrogen receptor expression in the normal and pre-cancerous breast. J Pathol 188:237–244. doi:10.1002/(SICI)1096-9896(199907)188:3<237::AID-PATH343>3.0.CO;2-8

9. Collaborative Group on Hormonal Factors in Breast Cancer (2004) Breast cancer and abortion: collaborative reanalysis of data from 53 epidemiological studies, including 83,000 with breast cancer from 16 countries. Lancet 363:1007–1016. doi:10.1016/S0140-6736(04)15835-2

10. Mote PA, Bartow S, Tran N, Clarke CL (2002) Loss of co-ordinate expression of progesterone receptors A and B is an early event in breast carcinogenesis. Breast Cancer Res Treat 72:163–172. doi:10.1023/A:1014820500738

11. Longacre TA, Bartow SA (1986) A correlative morphologic study of human breast and endometrium in the menstrual cycle. Am J Surg Pathol 10:382–393. doi:10.1097/00000478-19860 6000-00003

12. Speirs V, Skliris GP, Burdall SE, Carder PJ (2002) Distinct expression patterns of ER alpha and ER beta in normal human mammary gland. J Clin Pathol 55:371–374

13. Couse JF, Korach KS (1999) Estrogen receptor null mice: what have we learned and where will they lead us? Endocr Rev 20:358–417. doi:10.1210/er.20.3.358

14. Petersen OW, Hoyer PE, van Deurs B (1987) Frequency and distribution of estrogen receptor-positive cells in normal, non-lactating human breast tissue. Cancer Res 47:5748–5751

15. Clarke RB, Howell A, Potten CS, Anderson E (1997) Dissociation between steroid receptor expression and cell proliferation in the human breast. Cancer Res 57:4987–4991

16. Bartow SA (1998) Use of the autopsy to study ontogeny and expression of the estrogen receptor gene in human breast. J Mammary Gland Biol Neoplasia 3:37–48. doi:10.1023/A:1026 641401184

17. Jacquemier JD, Hassoun J, Torrente M, Martin P-M (1990) Distribution of estrogen and progesterone receptors in healthy tissue adjacent to breast lesions at various stages-Immunohistochemical study of 107 cases. Breast Cancer Res Treat 15:109–117. doi:10.1007/BF01810783

18. Williams G, Anderson E, Howell A, Watson R, Coyne J, Roberts SA, Potten CS (1991) Oral contraceptive (OCP) use increases proliferation and decreases oestrogen receptor content of epithelial cells in the normal human breast. Int J Cancer 48:206–210. doi:10.1002/ijc.2910480209

19. Battersby S, Robertson BJ, Anderson TJ, King RJB, McPherson K (1992) Influence of menstrual cycle, parity and oral contraceptive use on steroid hormone receptors in normal breast. Br J Cancer 65:601–607

20. Söderqvist G, von Schoultz B, Tani E, Skoog L (1993) Estrogen and progesterone receptor content in breast epithelial cells from healthy women during the menstrual cycle. Am J Obstet Gynecol 168:874–879
21. Russo J, Ao X, Grill C, Russo IH (1999) Pattern of distribution of cells positive for estrogen receptor alpha and progesterone receptor in relation to proliferating cells in the mammary gland. Breast Cancer Res Treat 53:217–227. doi:10.1023/A:1006186719322
22. Lee S, Mohsin SK, Mao S, Hilsenbeck SG, Medina D, Allred DC (2006) Hormones, receptors, and growth in hyperplastic enlarged lobular units: early potential precursors of breast cancer. Breast Cancer Res 8:R6. doi:10.1186/bcr1367
23. Battersby S, Anderson TJ (1988) Proliferative and secretory activity in the pregnant and lactating human breast. Virchows Archiv A Pathol Anat 413:189–196
24. Suzuki R, Atherton AJ, O'Hare MJ, Entwistle A, Lakhani SR, Clarke C (2000) Proliferation and differentiation in the human breast during pregnancy. Differentiation 66:106–115. doi:10.1046/j.1432-0436.2000.660205.x
25. Olsson H, Jernström H, Alm P, Kreipe H, Ingvar C, Jönsson PE, Rydén S (1996) Proliferation of the breast epithelium in relation to menstrual cycle phase, hormonal use, and reproductive factors. Breast Cancer Res Treat 40:187–196. doi:10.1007/BF01806214
26. Longacre TA, Bartow SA (1986) A correlative morphologic study of human breast and endometrium in the menstrual cycle. Am J Surg Pathol 10:382–393. doi:10.1097/00000478-198606000-00003
27. Anderson TJ, Battersby S, King RJB, McPherson K, Going JJ (1989) Oral contraceptive use influences resting breast proliferation. Hum Pathol 20:1139–1144. doi:10.1016/0046-8177(89)90049-X
28. Williams G, Anderson E, Howell A, Watson R, Coyne J, Roberts SA, Potten CS (1991) Oral contraceptive (OCP) use increases proliferation and decreases oestrogen receptor content of epithelial cells in the normal human breast. Int J Cancer 48:206–210. doi:10.1002/ijc.2910480209
29. Feuerhake F, Sigg W, Höfter EA, Unterberger P, Welsch U (2003) Cell proliferation, apoptosis, and expression of Bcl-2 and Bax in non-lactating human breast epithelium in relation to the menstrual cycle and reproductive history. Breast Cancer Res Treat 77:37–48. doi:10.1023/A:1021119830269
30. Joshi K, Smith JA, Perusinghe N, Monoghan P (1986) Cell proliferation in the human mammary epithelium. Am J Pathol 124:199–206
31. Mote PA, Leary JA, Avery KA, Sandelin K, Chenevix-Trench G, kConfab Investigators, Kirk JA, Clarke CL (2004) Germ-line mutations in BRCA1 or BRCA2 in the normal breast are associated with altered expression of estrogen-responsive proteins and the predominance of progesterone receptor A. Genes Chromosomes Cancer 39:236–248. doi:10.1002/gcc.10321
32. Jacobsen BM, Richer JK, Sartorius CA, Horwitz KB (2003) Expression profiling of human breast cancers and gene regulation by progesterone receptors. J Mammary Gland Biol Neoplasia 8:257–268. doi:10.1023/B:JOMG.0000010028.48159.84
33. Shyamala G, Yang X, Silberstein G, Barcellos-Hoff MH, Dale E (1998) Transgenic mice carrying an imbalance in the native ratio of A to B forms of progesterone receptor exhibit developmental abnormalities in mammary glands. Proc Natl Acad Sci USA 95:696–701. doi:10.1073/pnas.95.2.696
34. Graham JD, Yeates C, Balleine RL, Harvey SS, Milliken JS, Bilous AM, Clarke CL (1995) Characterization of progesterone receptor A and B expression in human breast cancer. Cancer Res 55:5063–5068